Inviscid instability of an incompressible flow between rotating porous cylinders to three-dimensional perturbations

Konstantin Ilin[a,*], Andrey Morgulis[b,c]

[a]*Department of Mathematics, University of York, Heslington, York YO10 5DD, UK*
[b]*Department of Mathematics, Mechanics and Computer Science, The Southern Federal University, Rostov-on-Don, Russian Federation*
[c]*South Mathematical Institute, Vladikavkaz Center of RAS, Vladikavkaz, Russian Federation*

Abstract

We consider the stability of the Couette-Taylor flow between porous cylinders with radial throughflow in the limit of high radial Reynolds number. It has already been shown earlier that this flow can be unstable to two-dimensional perturbations. In the present paper, we study its stability to general three-dimensional perturbations. In the limit of high radial Reynolds number, we show the following: (i) the purely radial flow is stable (for both possible directions of the flow); (ii) all rotating flows are stable with respect to axisymmetric perturbations; (iii) the instability occurs for both directions of the radial flow provided that the ratio of the azimuthal component of the velocity to the radial one at the cylinder, through which the fluid is pumped in, is sufficiently large; (iv) the most unstable modes are always two-dimensional, i.e. two-dimensional modes become unstable at the smallest ratio of the azimuthal velocity to the radial one; (v) the stability is almost independent of the rotation of the cylinder, through which the fluid is being pumped out. We extend these results to high but finite radial Reynolds numbers by means of an asymptotic expansion of the corresponding eigenvalue problem. Calculations of the first-order corrections show that small viscosity always enhances the flow stability. It is also shown that the asymptotic results give good approximations to the viscous eigenvalues even for moderate values of radial Reynolds number.

Keywords: instability, inviscid Couette-Taylor flow, radial flow
PACS: 47.20.Cq
2000 MSC: 76E07

1. Introduction

We consider the stability of a steady viscous incompressible flow in a gap between two rotating porous cylinders in the limit of high radial Reynolds number R (constructed using the radial velocity and the radius of the inner cylinder). The basic flow is rotationally and translationally (along the common axis of the cylinders) invariant and generalises the classical Couette-Taylor flow to the case when a radial flow is present. The direction of the radial flow can be from the inner cylinder to the outer one (the diverging flow) or from the outer cylinder to the inner one (the converging flow). It has been shown earlier [1, 2] that this flow can be unstable to small two-dimensional perturbations, and the aim of the present paper is to understand what happens if three-dimensional perturbations are allowed.

The stability of viscous flows between permeable rotating cylinders with a radial flow had been studied by many authors [3, 4, 5, 6, 7, 8, 9]. One of the main aims of these papers was to determine the effect of the radial flow on the stability of the circular Couette-Taylor flow to axisymmetric perturbations, and the general conclusion was that the radial flow affects the stability of the basic flow: both a converging radial flow and a sufficiently strong diverging flow have a stabilizing effect on the Taylor instability, but when a diverging flow is weak, it has a destabilizing effect [5, 6]. However, it was not clear whether a radial flow itself can induce instability for flows which are stable without it. This question had been answered affirmatively by Fujita et al [10] and later by Gallet et al [11] who had demonstrated

that particular classes of viscous flows between porous rotating cylinders can be unstable to small two-dimensional perturbations.

Later it had been shown by Ilin & Morgulis [1] that both converging and diverging irrotational flows can be linearly unstable to two-dimensional perturbations in the limit $R \to \infty$ and that the instability persists if small viscosity is taken into account. In Ref. [2], the same limit had been considered for general viscous flows between porous cylinders with a radial flow, and it had been shown that not only the particular classes of viscous steady flows considered in [11, 1] can be unstable to two-dimensional perturbations, but this is also true without any restriction on angular velocities of the cylinders and for both converging and diverging flows. A further development of the two-dimensional theory can be found in a recent paper by Kerswell [12] where, among other things, the effects of compressibility and nonlinearity have been considered. Kerswell has also pointed to a similarity between the instability induced by the radial flow and the so-called stratorotational instability (SRI) which is due to the axial density stratification of in the Couette-Taylor flow (see also [13]).

An interesting and important feature of the basic steady flow considered here is that it strongly depends on the radial Reynolds number R and on the direction of the radial flow. When $R = 0$ (no radial flow), it reduces to the standard Couette-Taylor flow, but when $R \gg 1$, it tends to an inviscid irrotational flow in which both radial and azimuthal components of the velocity are inversely proportional to r (where r is the radial coordinate of the polar cylindrical coordinate system). The parameters of this inviscid flow are determined by the radial and azimuthal components of the velocity at the flow inlet (i.e. at the inner cylinder for the diverging flow or at the outer cylinder for the converging flow) irrespective of what happens at the outlet. This means that a single inviscid flow represents the inviscid limit common for all viscous flows with the same radial mass flux and the same azimuthal velocity at the inlet irrespective of the angular velocity of the other cylinder (which represents the flow outlet). Of course, the inviscid flow approximates the exact viscous flow only outside a thin boundary layer near the flow outlet, and the boundary layer depends on the angular velocity of the other cylinder. However, an asymptotic expansion for $R \gg 1$, constructed in [2] for the two-dimensional problem, shows that the leading term is completely determined by the inviscid stability problem for the basic inviscid flow described above and does not depend on the boundary layer. Interestingly, the first viscous correction term in the expansion also does not depend on the details of the boundary layer in the basic flow, i.e. the first viscous correction does not feel what is happening at the flow outlet.

In the present paper, we examine the effect of three-dimensional perturbations on the stability properties of the basic flow described above for the flow regimes with high radial Reynolds number. We construct an asymptotic expansion of the eigenvalue problem for normal modes for $R \gg 1$, study the inviscid problem in detail and compute the principal viscous corrections to the inviscid eigenvalues. In particular, we rigorously prove that axisymmetric inviscid modes always decay exponentially, as well as all inviscid modes for the purely radial basic flow. The critical curves of the inviscid instability computed numerically show that, for a wide range of the flow parameters and for both diverging and converging flows, the unstable inviscid modes appear as soon as the circulation of the velocity at the flow inlet becomes larger that a certain critical value and that the purely two-dimensional azimuthal waves are always the most unstable ones, i.e. they correspond to the smallest critical value of the inlet circulation. At the same time, the instability is almost independent of the azimuthal velocity at the outlet. This means that the Couette-Taylor flow in the presence of the radial flow can be unstable far beyond the Rayleigh line (that separates inertially stable and unstable regimes in the classical Couette-Taylor flow).

We also calculate viscous corrections and investigate their effect on the instability. In particular, the analysis of the principal viscous corrections shows that, for both the diverging and converging flows, small viscosity always enhances the flow stability.

The outline of the paper is as follows. In Section 2, we discuss the exact viscous basic flow and its inviscid limit and formulate the exact and inviscid linear stability problems. Section 3 contains a linear inviscid stability analysis of both the diverging and converging flows basic flows. In Section 4, the effect of viscosity is considered. Discussion of the results is presented in Section 5.

2. Formulation of the problem

2.1. Exact equations and basic steady flow

We consider three-dimensional viscous incompressible flows in the gap between two concentric circular cylinders with radii r_1 and r_2 ($r_2 > r_1$). The cylinders are permeable for the fluid and there is a constant volume flux $2\pi Q$ (per

unit length measured along the common axis of the cylinders) of the fluid through the gap (the fluid is pumped into the gap at the inner cylinder and taken out at the outer one or *vice versa*). Q will be positive if the direction of the flow is from the inner cylinder to the outer one and negative if the flow direction is reversed. Flows with positive and negative Q will be referred to as diverging and converging flows respectively. Suppose that r_1 is taken as a length scale, $r_1^2/|Q|$ as a time scale, $|Q|/r_1$ as a scale for the velocity and $\rho Q^2/r_1^2$ for the pressure where ρ is the fluid density. Then the Navier-Stokes equations, written in non-dimensional variables, have the form

$$u_t + uu_r + \frac{v}{r}u_\theta + wu_z - \frac{v^2}{r} = -p_r + \frac{1}{R}\left(\nabla^2 u - \frac{u}{r^2} - \frac{2}{r^2}v_\theta\right), \tag{1}$$

$$v_t + uv_r + \frac{v}{r}v_\theta + wu_z + \frac{uv}{r} = -\frac{1}{r}p_\theta + \frac{1}{R}\left(\nabla^2 v - \frac{v}{r^2} + \frac{2}{r^2}u_\theta\right), \tag{2}$$

$$w_t + uw_r + \frac{v}{r}w_\theta + ww_z = -p_z + \frac{1}{R}\nabla^2 w, \tag{3}$$

$$\frac{1}{r}(ru)_r + \frac{1}{r}v_\theta + w_z = 0. \tag{4}$$

Here (r, θ, z) are the polar cylindrical coordinates, u, v and w are the radial, azimuthal and axial components of the velocity, p is the pressure, $R = |Q|/\nu$ is the Reynolds number (ν is the kinematic viscosity of the fluid); subscripts denote partial derivatives; ∇^2 is the polar form of the Laplace operator:

$$\nabla^2 = \partial_r^2 + \frac{1}{r}\partial_r + \frac{1}{r^2}\partial_\theta^2 + \partial_z^2.$$

We employ the following boundary conditions

$$u\big|_{r=1} = \beta, \quad u\big|_{r=a} = \frac{\beta}{a}, \quad v\big|_{r=1} = \gamma_1, \quad v\big|_{r=a} = \frac{\gamma_2}{a}, \quad w\big|_{r=1} = w\big|_{r=a} = 0 \tag{5}$$

where

$$a = \frac{r_2}{r_1}, \quad \beta = \frac{Q}{|Q|}, \quad \gamma_1 = \frac{\Omega_1 r_1^2}{|Q|}, \quad \gamma_2 = \frac{\Omega_2 r_2^2}{|Q|},$$

with Ω_1 and Ω_2 being the angular velocities of the inner and outer cylinders respectively. Parameter β takes values $+1$ or -1 which correspond to the diverging and converging flows respectively; γ_1 and γ_2 represent the ratio of the azimuthal component of the velocity to the radial one at the inner and outer cylinders respectively. Boundary condition (5) prescribe all components of the velocity at the cylinders and model conditions on the interface between a fluid and a porous wall [14].

The only steady rotationally symmetric and translationally invariant (in the z direction) solution of problem (1)–(5) is given by

$$u = \frac{\beta}{r}, \quad v = V(r) = Ar^{\beta R+1} + \frac{B}{r}, \quad P = -\frac{1}{2r^2} + \int \frac{V^2(r)}{r}\,dr \tag{6}$$

where

$$A = \frac{\gamma_2 - \gamma_1}{a^{\beta R+2} - 1}, \quad B = \frac{a^{\beta R+2}\gamma_1 - \gamma_2}{a^{\beta R+2} - 1}. \tag{7}$$

This solution is well defined for all $\beta R \neq -2$. For $\beta R = -2$, the solution is given by

$$u = -\frac{1}{r}, \quad v = V(r) = \widetilde{A}\frac{\ln r}{r} + \frac{\widetilde{B}}{r} \tag{8}$$

where

$$\widetilde{A} = \frac{\gamma_2 - \gamma_1}{\ln a}, \quad \widetilde{B} = \gamma_1.$$

The azimuthal velocity profile has a non-trivial dependence on R. When $R = 0$ (no radial flow), it reduces to the classical Couette-Taylor profile, $V(r) = Ar + B/r$. When $R \to \infty$, the limit depends on β, i.e. on the direction of the

3

radial flow. It can be shown (see [2]) that, for $R \gg 1$, the azimuthal component of the velocity is well approximated by

$$V(r) = \begin{cases} \gamma_1/r + f(\eta)/a + O\left(R^{-1}\right) & \text{for } \beta = 1 \\ \gamma_2/r - f(\xi) + O\left(R^{-1}\right) & \text{for } \beta = -1 \end{cases} \tag{9}$$

where $\eta = R(1 - r/a)$ and $\xi = R(r - 1)$ are the boundary layer variables (at the outer and inner cylinders respectively) and function f is defined as

$$f(s) = (\gamma_2 - \gamma_1)\, e^{-s}. \tag{10}$$

Equations (9) and (10) mean that, in the limit of high Reynolds numbers, the flow becomes *irrotational and proportional to r^{-1} everywhere except for a thin boundary layer near the outflow part of the boundary* (i.e. near the outer cylinder for the diverging flow and the inner cylinder for the converging flow). The boundary layer thickness is $O(R^{-1})$. Note that there is no boundary layer at the inflow part of the boundary. This is consistent with the general theory of flows through a given domain with permeable boundary in the limit of vanishing viscosity (see, e.g., [15, 16, 17, 18]).

If the boundary layer is ignored, we obtain the corresponding inviscid flow:

$$u = \frac{\beta}{r}, \quad v = \begin{cases} \gamma_1/r & \text{for } \beta = 1 \\ \gamma_2/r & \text{for } \beta = -1 \end{cases} \tag{11}$$

It is a remarkable fact that the single inviscid flow (11) represents the high-Reynolds-number limit for each member of a one-parameter family of viscous flows (6) (parametrised by γ_2 for $\beta = 1$ and by γ_1 for $\beta = -1$).

The inviscid flow (11) is the only steady rotationally symmetric and translationally invariant (in the z direction) solution of the Euler equations that satisfies the boundary conditions

$$u\big|_{r=1} = \beta, \quad u\big|_{r=a} = \frac{\beta}{a}, \quad v\big|_{r=1} = \gamma_1, \quad w\big|_{r=1} = 0 \tag{12}$$

for $\beta = 1$ (the diverging flow) and

$$u\big|_{r=1} = \beta, \quad u\big|_{r=a} = \frac{\beta}{a}, \quad v\big|_{r=a} = \frac{\gamma_2}{a}, \quad w\big|_{r=a} = 0 \tag{13}$$

for $\beta = -1$ (the converging flow). Note that the boundary conditions at the inflow part of the boundary include all components of the velocity (not only the normal one as in the case of impermeable boundary). These boundary conditions are special ones because (i) they lead to a well-posed mathematical problem (see, e.g., [19]) and (ii) they are consistent with the vanishing viscosity limit for the Navier-Stokes equations (see, e.g., [15, 16]). It should be mentioned that, in the literature, one can find other types of boundary condition employed for inviscid flows through a domain with permeable boundary (see, e.g. [19, 20]). Some of these alternative boundary conditions lead to mathematically well-posed problems. However, only the conditions described above are consistent with the vanishing viscosity limit for the Navier-Stokes equations (1)–(4) with boundary conditions (5).

We note in passing that the uniqueness of the steady inviscid flow (11) may look strange if we ignore the viscosity from the very beginning. This is because of the following 'paradox': if there were no radial flow, there would exist infinitely many steady inviscid flows satisfying boundary conditions (12) or (13) with arbitrary azimuthal velocity $v = V(r)$. However, only one solution is possible in the presence of the radial flow. This 'paradox' can be explained by solving an initial value problem for the Euler equation with boundary conditions (12) or (13). Adding a steady radial flow for $t > 0$ to an initial velocity which is purely azimuthal $\mathbf{v} = V(r)\mathbf{e}_\theta$ with any $V(r)$ will produce the inviscid flow (11) after a finite time when all the fluid particles which were in the flow domain initially are washed out of it by the radial flow.

The classical Couette-Taylor flow ($R = 0$) is centrifugally unstable to inviscid axisymmetric perturbations if the Rayleigh discriminant, given by $\Phi(r) = r^{-3}d(rV(r))^2/dr$, is negative somewhere in the flow and stable if $\Phi(r) > 0$ for all $1 < r < a$.[1] According to the Rayleigh criterion, the Couette-Taylor flow is always unstable if γ_1 and γ_2 have

---

[1] Although there is no evidence suggesting that the Couette-Taylor flow may be unstable to non-aixisymmetric perturbations if $\Phi(r) > 0$ for all $1 < r < a$, it has never been formally proved (except for the case of large axial wavenumbers [21]).

4

different signs. For positive γ_1 and γ_2, the regions of stable and unstable Couette-Taylor flows are separated by the Rayleigh line, $\gamma_2 = \gamma_1$ (which bicests the first quadrant of the (γ_1, γ_2) plane). Although the Couette-Taylor flow with radial crossflow for $R > 0$ is different from the classical Couette-Taylor flow, the Rayleigh discriminant has the same properties for $\beta = \pm 1$ and any R: $\Phi(r) > 0$ (for $0 < r < a$) if $\gamma_1 < \gamma_2$, $\Phi(r) < 0$ (for $0 < r < a$) if $\gamma_1 > \gamma_2$, and $\Phi(r) \equiv 0$ for $\gamma_1 = \gamma_2$. However, as will be demonstrated below, the presence of the radial crossflow radically changes the stability properties of the Couette-Taylor flow: any flow with sufficiently large γ_1 and γ_2 turns out to be unstable in the limit of high radial Reynolds numbers irrespective of whether γ_1 is smaller or larger than γ_2. This means that the Rayleigh criterion is not relevant for the basic flow (6) at least when $R \gg 1$.

2.2. Linear stability problem

We will consider a small perturbation $(\tilde{u}, \tilde{v}, \tilde{w}, \tilde{p})$ of the basic flow (6) in the form of the normal mode

$$\{\tilde{u}, \tilde{v}, \tilde{w}, \tilde{p}\} = Re\left[\{\hat{u}(r), \hat{v}(r), \hat{w}(r), \hat{p}(r)\}e^{\sigma t + in\theta + ikz}\right] \tag{14}$$

where $n \in \mathbb{Z}$ and $\sigma \in \mathbb{C}$. This leads to the eigenvalue problem for σ:

$$\left(\sigma + \frac{inV}{r} + \frac{\beta}{r}\partial_r\right)\hat{u} - \frac{\beta}{r^2}\hat{u} - \frac{2V}{r}\hat{v} = -\partial_r\,\hat{p} + \frac{1}{R}\left(L\hat{u} - \frac{\hat{u}}{r^2} - \frac{2in}{r^2}\hat{v}\right), \tag{15}$$

$$\left(\sigma + \frac{inV}{r} + \frac{\beta}{r}\partial_r\right)\hat{v} + \frac{\beta}{r^2}\hat{v} + \Omega(r)u = -\frac{in}{r}\,\hat{p} + \frac{1}{R}\left(L\hat{v} - \frac{\hat{v}}{r^2} + \frac{2in}{r^2}\hat{u}\right), \tag{16}$$

$$\left(\sigma + \frac{inV}{r} + \frac{\beta}{r}\partial_r\right)\hat{w} = -ik\,\hat{p} + \frac{1}{R}\,L\hat{w}, \tag{17}$$

$$\partial_r\,(r\hat{u}) + in\,\hat{v} + ikr\,\hat{w} = 0, \tag{18}$$

$$\hat{u}(1) = 0, \quad \hat{u}(a) = 0, \quad \hat{v}(1) = 0, \quad \hat{v}(a) = 0, \quad \hat{w}(1) = 0, \quad \hat{w}(a) = 0. \tag{19}$$

In Eqs. (15)–(19),

$$L = \frac{d^2}{dr^2} + \frac{1}{r}\frac{d}{dr} - \left(k^2 + \frac{n^2}{r^2}\right), \quad \Omega(r) = V'(r) + \frac{V(r)}{r}.$$

Equations (15)–(19) represent an eigenvalue problem for σ. If there is an eigenvalue σ such that $Re(\sigma) > 0$, then the basic flow is unstable. If there are no eigenvalues with positive real part and if there are no perturbations with non-exponential growth (examples of non-exponential growth can be found, e.g., in [22]), then the flow is linearly stable. Although the possibility of the non-exponentially growing perturbations certainly deserves attention especially in the limit of the vanishing viscosity, this question is beyond the scope of this paper. For $k = 0$, problem (15)–(19) reduces to the two-dimensional viscous stability problem that had been studied in [2].

We are interested in the asymptotic behaviour of the solutions to this eigenvalue problem for high Reynolds numbers R ($R \gg 1$) and, especially, in the effect of the three-dimensionality on the stability properties of the flow. In the limit $R \to \infty$, Eqs. (15)–(17) formally reduce to

$$\left(\sigma + \frac{in\gamma}{r^2} + \frac{\beta}{r}\partial_r\right)\hat{u} - \frac{\beta}{r^2}\hat{u} - \frac{2\gamma}{r^2}\hat{v} = -\partial_r\,\hat{p}, \tag{20}$$

$$\left(\sigma + \frac{in\gamma}{r^2} + \frac{\beta}{r}\partial_r\right)\hat{v} + \frac{\beta}{r^2}\hat{v} = -\frac{in}{r}\,\hat{p}, \tag{21}$$

$$\left(\sigma + \frac{in\gamma}{r^2} + \frac{\beta}{r}\partial_r\right)\hat{w} = -ik\,\hat{p} \tag{22}$$

where γ is the (dimensionless) circulation at the flow inlet, defined by

$$\gamma = \begin{cases} \gamma_1 & \text{for } \beta = 1 \\ \gamma_2 & \text{for } \beta = -1 \end{cases}$$

These equations and Eq. (18) describe the normal mode solutions of the Euler equations linearised on the steady inviscid flow (11). Following the above discussion of the inviscid boundary conditions, we drop the conditions for the

tangent components of the velocity at the outlet from viscous boundary conditions (19). As a result, we obtain the following conditions for $\hat{u}$, $\hat{v}$ and $\hat{w}$:

$$\hat{u}(1) = \hat{u}(a) = 0, \quad \hat{v}(1) = 0, \quad \hat{w}(1) = 0 \tag{23}$$

for $\beta = 1$ (the diverging flow) and

$$\hat{u}(1) = \hat{u}(a) = 0, \quad \hat{v}(a) = 0, \quad \hat{w}(a) = 0 \tag{24}$$

for $\beta = -1$ (the converging flow).

Later we will see that the inviscid eigenvalue problem (20)–(24), (18) describes the leading term of an asymptotic expansion of the viscous eigenvalue problem (15)–(19) for high radial Reynolds numbers ($R \gg 1$). This asymptotic expansion as well as a discussion of viscous effects will be presented in section 4. Before that, we will consider the inviscid problem.

3. Analysis of the inviscid eigenvalue problem

It is convenient to rewrite Eqs. (20)–(22) in the terms of perturbation vorticity

$$\hat{\boldsymbol{\omega}} = \hat{\omega}_1\,\mathbf{e}_r + \hat{\omega}_2\,\mathbf{e}_\theta + \hat{\omega}_3\,\mathbf{e}_z \tag{25}$$

where $\mathbf{e}_r$, $\mathbf{e}_\theta$ and $\mathbf{e}_z$ are unit vectors in the radial, azimuthal and axial directions, respectively, and where

$$\hat{\omega}_1 = \frac{in}{r}\,\hat{w} - ik\hat{v}, \tag{26}$$

$$\hat{\omega}_2 = ik\hat{u} - \hat{w}_r, \tag{27}$$

$$\hat{\omega}_3 = \frac{1}{r}\,(r\hat{v})_r - \frac{in}{r}\,\hat{u}. \tag{28}$$

Applying operator *curl* to Eqs. (20)–(22), we obtain

$$\left(h(r) + \frac{\beta}{r}\,\partial_r\right)(r\hat{\omega}_1) = 0, \tag{29}$$

$$\left(h(r) + \frac{\beta}{r}\,\partial_r\right)\left(\frac{\hat{\omega}_2}{r}\right) = -\frac{2\gamma}{r^3}\,\omega_1, \tag{30}$$

$$\left(h(r) + \frac{\beta}{r}\,\partial_r\right)\hat{\omega}_3 = 0 \tag{31}$$

where

$$h(r) = \sigma + \frac{in\gamma}{r^2}. \tag{32}$$

Equations (29)–(31) should be solved subject to the boundary conditions (23) for the diverging flow and (24) for the converging flow.

The eigenvalue problem (29)–(31) and (23) or (24) can be reduced to a problem of finding zeros of a certain entire function. We will show this first for the divergent flow.

3.1. Diverging flow ($\beta = 1$)

3.1.1. Dispersion relation

Boundary conditions (23) and Eq. (26) imply that

$$\hat{\omega}_1\big|_{r=1} = 0. \tag{33}$$

Now let

$$g(r) = \sigma\,\frac{r^2}{2} + in\gamma\,\ln r, \tag{34}$$

6

so that $h(r)$, given by (32), can be written as $h(r) = g'(r)/r$. Then the general solution of Eq. (29) is

$$r\hat{\omega}_1 = Ce^{-g(r)}$$

where C is an arbitrary constant. This and Eq. (33) imply that $C = 0$ and, therefore, $\hat{\omega}_1(r) = 0$, so that we have the relation

$$\frac{in}{r}\hat{w} - ik\hat{v} = 0. \tag{35}$$

Now we assume that $n \neq 0$. The case of $n = 0$ will be treated separately. Using (35) to eliminate $\hat{w}$ from the incompressibility condition (18), we obtain

$$\frac{in}{r}(r\hat{u})_r - \left(k^2 + \frac{n^2}{r^2}\right)r\hat{v} = 0. \tag{36}$$

Integration of Eq. (31) yields

$$\hat{\omega}_3 = C_1 e^{-g(r)} \tag{37}$$

for an arbitrary constant C_1. Equations (37) and (28) have a consequence that

$$inr\hat{u} = r(r\hat{v})_r - C_1 r^2 e^{-g(r)}. \tag{38}$$

Finally, we use (38) to eliminate $\hat{u}$ from Eq. (36). As a result, we get the equation

$$G_{rr} + \frac{1}{r}G_r - \left(k^2 + \frac{n^2}{r^2}\right)G = C_1 F(r) \tag{39}$$

where

$$G(r) = r\hat{v}(r) \tag{40}$$

and

$$F(r) = \frac{1}{r}\partial_r\left(r^2 e^{-g(r)}\right). \tag{41}$$

Equation (38) allows us to rewrite boundary conditions (23) (for $\hat{u}$ and $\hat{v}$) in terms of G:

$$G(1) = 0, \tag{42}$$
$$G'(1) = C_1 e^{-g(1)}, \tag{43}$$
$$G'(a) = C_1 a e^{-g(a)}. \tag{44}$$

Equation (39) together with boundary conditions (42)–(44) represent an eigenvalue problem for σ (that enters the problem via $g(r)$).

The general solution of Eq. (39) can be written as

$$G(r) = C_1 \int_1^r F(s)\left[I_n(kr)K_n(ks) - I_n(ks)K_n(kr)\right]s\,ds + C_2 I_n(kr) + C_3 K_n(kr). \tag{45}$$

Here $I_n(z)$ and $K_n(z)$ are the modified Bessel functions of the first and second kind; C_2 and C_3 are arbitrary constants (recall that C_1 is also arbitrary). Substitution of the general solution into boundary conditions (42) and (43) results in the following two equations:

$$C_2 I_n(k) + C_3 K_n(k) = 0,$$
$$C_2 kI'_n(k) + C_3 kK'_n(k) = C_1 e^{-g(1)}.$$

Solving these for C_1 and C_2, we obtain

$$C_2 = C_1 K_n(k)e^{-g(1)}, \quad C_3 = -C_1 I_n(k)e^{-g(1)}. \tag{46}$$

Here we have used the Wronskian relation (e.g. [23]):

$$I'_n(z)K_n(z) - I_n(z)K'_n(z) = \frac{1}{z}. \tag{47}$$

With the help of (46), we can rewrite Eq. (45) in the form

$$G(r) = C_1 \left\{ \int_1^r F(s) \left[I_n(kr)K_n(ks) - I_n(ks)K_n(kr) \right] s\, ds + \left[I_n(kr)K_n(k) - I_n(k)K_n(kr) \right] e^{-g(1)} \right\}.$$

Substituting this into boundary condition (44), we obtain the dispersion relation

$$\int_1^a F(s)k \left[I'_n(ka)K_n(ks) - I_n(ks)K'_n(ka) \right] s\, ds$$

$$+ k \left[I'_n(ka)K_n(k) - I_n(k)K'_n(ka) \right] e^{-g(1)} - a\, e^{-g(a)} = 0. \tag{48}$$

This dispersion relation can be further simplified as follows. Let $\mathcal{I}$ be the integral entering the dispersion relation. Recalling that $F(r)$ is given by Eq. (41) and integrating by parts, we obtain

$$
\begin{aligned}
\mathcal{I} \;=\;& k \int_1^a \frac{1}{s} \partial_s \left(s^2 e^{-g(s)} \right) \left[I'_n(ka)K_n(ks) - I_n(ks)K'_n(ka) \right] s\, ds \\
\;=\;& s^2 e^{-g(s)} k \left[I'_n(ka)K_n(ks) - I_n(ks)K'_n(ka) \right] \Big|_1^a \\
&- k^2 \int_1^a e^{-g(s)} \left[I'_n(ka)K'_n(ks) - I'_n(ks)K'_n(ka) \right] s^2\, ds \\
\;=\;& a e^{-g(a)} - e^{-g(1)} k \left[I'_n(ka)K_n(k) - I_n(k)K'_n(ka) \right] \\
&- k^2 \int_1^a e^{-g(s)} \left[I'_n(ka)K'_n(ks) - I'_n(ks)K'_n(ka) \right] s^2\, ds.
\end{aligned}
$$

Here again we have used the Wronskian relation (47). Substitution of the above formula for $\mathcal{I}$ into (48) yields the final expression for the dispersion relation:

$$D(\sigma, n, k, \gamma, a) \equiv k^2 \int_1^a e^{-\sigma s^2/2 - in\gamma \ln s} \left[I'_n(ks)K'_n(ka) - I'_n(ka)K'_n(ks) \right] s^2\, ds = 0. \tag{49}$$

It can be shown that in the limit $k \to 0$ this reduces to the dispersion relation of the corresponding two-dimensional problem (considered in [1]).

The dispersion relation (49) has been obtained under assumption that $n \neq 0$. Nevertheless, it can be shown that this dispersion relation is also valid for the axisymmetric mode, $n = 0$.

The eigenfunction $G(r)$ associated with the eigenvalue σ can be written as

$$G(r) = C_1 k \int_1^r e^{-\sigma s^2/2 - in\gamma \ln s} \left[I'_n(ks)K_n(kr) - I_n(kr)K'_n(ks) \right] s^2\, ds,$$

while the corresponding formula for $H(r) \equiv r\hat{u}(r)$ is

$$H(r) = C_1 \frac{k^2}{in} r \int_1^r e^{-\sigma s^2/2 - in\gamma \ln s} \left[I'_n(ks)K'_n(kr) - I'_n(kr)K'_n(ks) \right] s^2\, ds.$$
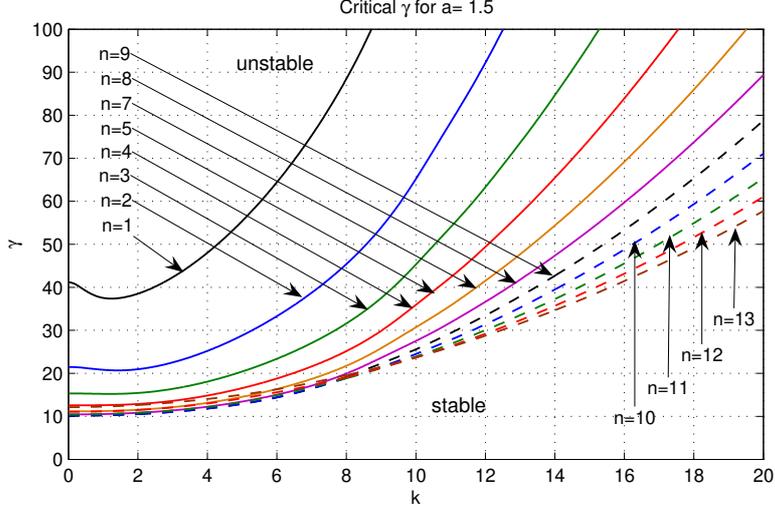
8

Figure 1: Neutral curves for $\beta = 1$ (diverging flow), $a = 1.5$ and $n = 1, \ldots, 13$. The region above each curve is where the corresponding mode is unstable.

3.1.2. General properties of the dispersion relations (49)

It has been mentioned in [24] that certain conclusions about a two-dimensional counterpart of (49) can be made using the Pólya theorem (see problem 177 of Part V in [25], see also [26]). It turns out that this theorem also works for (49). It is shown in Appendix A that, for the purely radial flow ($\gamma = 0$), the dispersion relation (49) has no roots with non-negative real part, so that there are no growing normal modes for the purely radial diverging flow. The same is true for the axisymmetric mode, $n = 0$ (see Appendix A). So, we can restrict our attention to non-axisymmetric perturbations for $\gamma \neq 0$.

Also, using the fact that $I_{-n}(z) = I_n(z)$ and $K_{-n}(z) = K_n(z)$ (e.g. [23]), we deduce from (49) that

$$\overline{D(\sigma, n, k, a, \gamma)} = D(\bar{\sigma}, -n, k, a, \gamma), \tag{50}$$

$$D(\sigma, n, k, a, \gamma) = D(\sigma, -n, k, a, -\gamma) \tag{51}$$

where the bar denotes complex conjugation. These relations imply that it suffices to consider only positive n and γ.

3.1.3. Numerical results

As we already know, for $\gamma = 0$, all eigenvalues lie in the left half-plane of complex variable σ. Numerical evaluation of (49) confirms this fact and shows that when γ increases from 0, some eigenvalues move to the right, and there is a critical value $\gamma_{cr} > 0$ of parameter γ at which one of the eigenvalues crosses the imaginary axis, so that

$$\mathrm{Re}(\sigma) > 0 \ \text{ for } \ \gamma > \gamma_{cr} \ \text{ and } \ \mathrm{Re}(\sigma) < 0 \ \text{ for } \ \gamma < \gamma_{cr}.$$

We have computed neutral curves ($\mathrm{Re}(\sigma) = 0$) on the (k, γ) plane for several values of the geometric parameter a and for $n = 1, 2, \ldots 20$. For all a, the neutral curves look qualitatively similar to what is shown in Fig. 1. One can see that the neutral curves for a few modes with low azimuthal wave number can be non-monotonic functions of the axial wave number k (e.g., $n = 1, 2, 3$ in Fig. 1). However, all other modes are strictly increasing functions of k. Let $\Gamma(k)$ be the critical value of γ minimized over $n = 1, \ldots, 20$:

$$\Gamma(k) = \min_n \gamma_{cr}(n, k).$$

Functions $\Gamma(k)$ for several values of the geometric parameter a are shown in Fig. 2. This figure demonstrates the following three things. First, $\Gamma(k)$, for any value of the geometric parameter a, is an increasing function, so that its
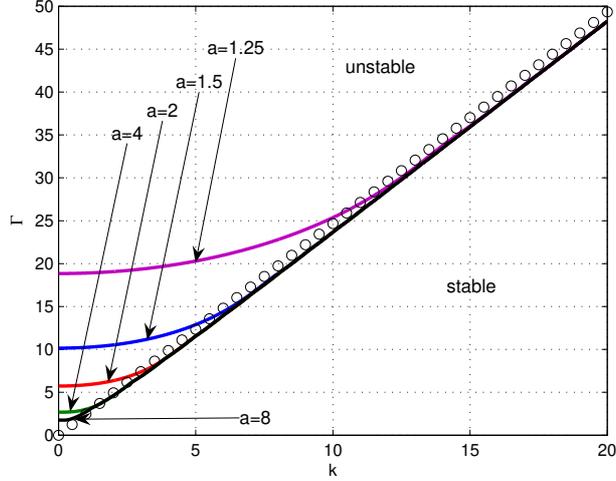
9

Figure 2: Critical γ minimized over azimuthal wave numbers $n = 1, 2, \ldots 20$ ($\Gamma = \min_n \gamma_{cr}$) for the diverging flow and $a = 1.25, 1.5, 2, 4, 8$. The region above each curve is where the corresponding flow is unstable. Circles show the asymptotic approximation to the stability boundary for large k derived in Appendix B.

minimum is attained at $k = 0$, i.e. for the two-dimensional mode. Thus the mode that becomes unstable first when γ increases from 0 (we will call it the most unstable mode) is two-dimensional. Second, for small to moderate values of k ($k \lesssim 10$), function $\Gamma(k)$ considerably depends on a: on one hand, it decreases when a is increased and seems to tend to a limit for large a; on the other hand, it grows when a tends to 1. Third, $\Gamma(k)$, for any value of a, becomes a linear function of k for sufficiently large k. Moreover, this linear asymptote is the same for all values of a. It is shown in Appendix B that in the limit of large k and n, more precisely, if

$$n = \alpha k \quad \text{and} \quad k \to \infty,$$

where α is a positive constant, then

$$\min_\alpha \gamma_{cr}(\alpha, k) \sim 2.4671\, k.$$

This asymptotic appriximation is shown by circles in Fig. 2. Evidently, it is in a good agreement with the numerical results. The azimuthal wave number n of the most unstable mode (that, for a fixed k, becomes unstable first when γ is increased from 0) depends on both a and k. The results of the numerical calculations of this quantity are shown in Fig. 3. The jumps in n correspond to the intersection points of the neutral curves for individual azimuthal modes. Figure 3 indicates that, for sufficiently large k, the azimuthal wave number of the most unstable mode, n, is independent of a and $n \sim k$. The graphs of the real and imaginary parts of functions $G(r)$ and $H(r)$ corresponding to the critical value of γ for $a = 2$ and $n = 4$ are shown in Figs. 4 and 5. Evidently, when the axial wave number increases, both $G(r)$ and $H(r)$ become more oscillatory. In addition to this, function $H(r)$ becomes concentrated near the inner cylinder (i.e. at the flow inlet). All the mentioned features observed numerically for relatively large k match the short-wave asymptotic described in the Appendix B.

3.2. Converging flow ($\beta = -1$)

3.2.1. Dispersion relation

An analysis similar to what we did for $\beta = 1$ results in the following dispersion relation

$$D_1(\sigma, n, k, \gamma, a) \equiv k^2 \int_1^a e^{\sigma s^2/2 + in\gamma \ln s} \left[I_n'(ks) K_n'(k) - I_n'(k) K_n'(ks) \right] s^2 \, ds = 0. \tag{52}$$
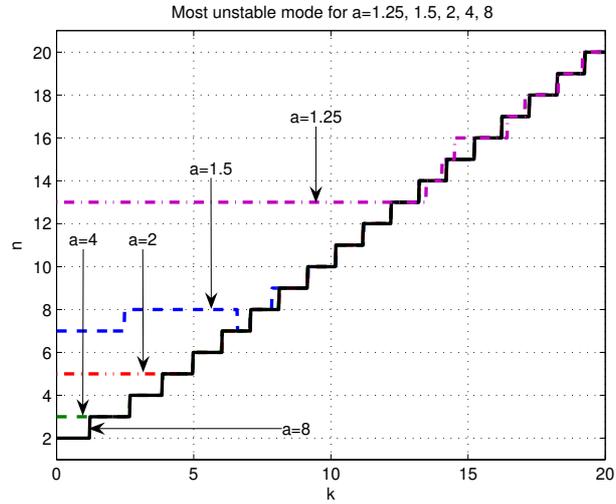
10

Figure 3: The azimuthal wave number of the most unstable mode, n, for the diverging flow as a function of k for $a = 1.25, 1.5, 2, 4, 8$.

Figure 4: Eigenfunction $G(r)$ for neutral modes ($\gamma = \gamma_{cr}$) for the diverging flow, $a = 2$ and $n = 4$: (a) $k = 1$, $\gamma = 5.9483$; (b) $k = 10$, $\gamma = 35.7645$; (c) $k = 20$, $\gamma = 128.2941$.
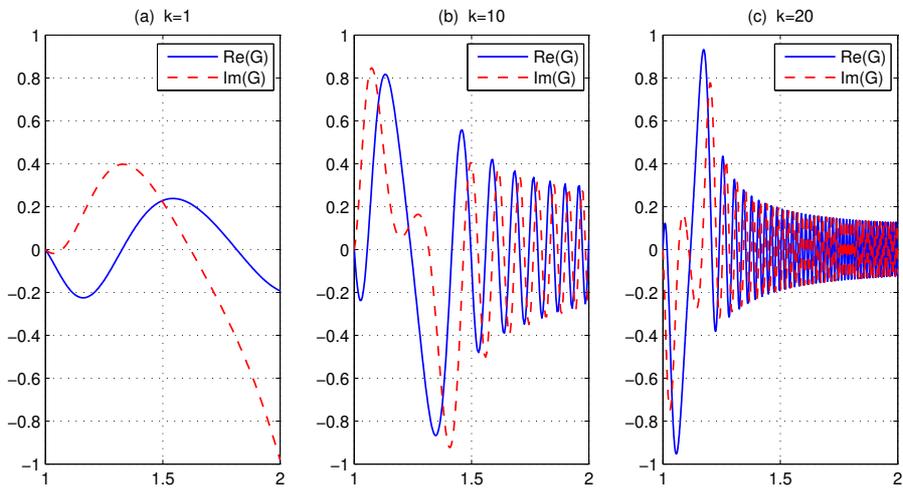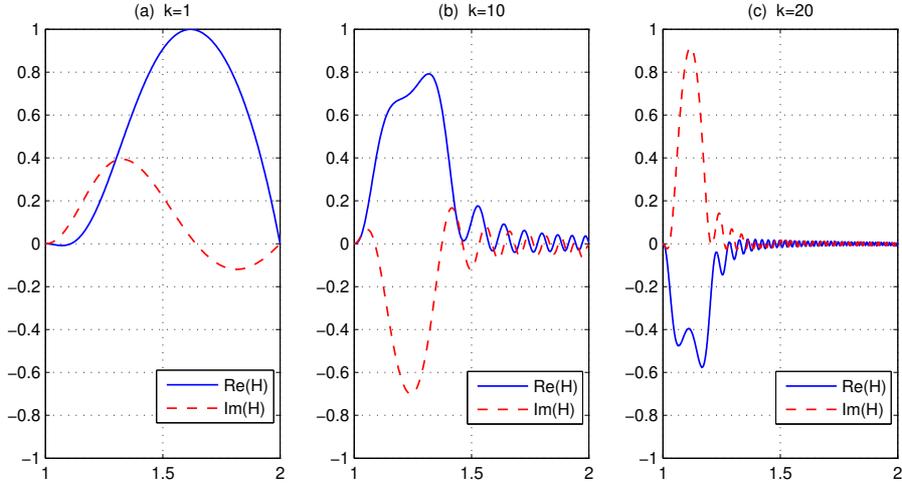
Figure 5: Eigenfunction $H(r)$ for neutral modes ($\gamma = \gamma_{cr}$) for the diverging flow, $a = 2$ and $n = 4$: (a) $k = 1$, $\gamma = 5.9483$; (b) $k = 10$, $\gamma = 35.7645$; (c) $k = 20$, $\gamma = 128.2941$.

Again, it can be shown that in the limit $k \to 0$ this reduces to the dispersion relation of the corresponding two-dimensional problem (see [1]).

Similarly to how this was done in Appendix B for the diverging flow, it can be shown that the dispersion relation (52) has no roots with non-negative real part (i) for the purely radial converging flow (i.e. for $\gamma = 0$ and for all n) and (ii) for the axisymmetric mode (for $n = 0$ and for all γ).

The dispersion relation (52) has the same symmetry properties as its counterpart (49) for the diverging flow:

$$\overline{D_1(\sigma, n, k, a, \gamma)} = D_1(\bar{\sigma}, -n, k, a, \gamma), \tag{53}$$

$$D_1(\sigma, n, k, a, \gamma) = D_1(\sigma, -n, k, a, -\gamma). \tag{54}$$

These relations imply that we need to consider only positive n and γ.

3.2.2. Numerical results

Numerical results for the converging flow are similar to those for the diverging flow: for $\gamma = 0$, all eigenvalues lie in the left half-plane of complex variable σ; when γ increases from 0, some eigenvalues move to the right and cross the imaginary axis. In the case of the converging flow, we will use parameter ka instead of k. This is convenient because, to a certain extent, it allows us to eliminate the dependence of the results on the geometric parameter a. We have computed neutral curves ($\text{Re}(\sigma) = 0$) on the (ka, γ) plane for several values of the geometric parameter a and for $n = 1, 2, \ldots 20$. For all a, the neutral curves look qualitatively similar to what is shown for $a = 1.5$ in Fig. 6. We have found that, at least for $a = 1.25, 1.5, 2, 4$ and 8, the neutral curves for all azimuthal modes are increasing functions of k (this differs from the case of the diverging flow where neutral curves for some low azimuthal modes can have a local minimum, e.g. for the modes with $n = 1, 2$ in Fig. 1). Function $\Gamma(ka) = \min_n \gamma_{cr}(n, ka)$ for several values of the geometric parameter a is shown in Fig. 7, and the azimuthal wave number of the most unstable mode, n (that, for a fixed ka, becomes unstable first when γ it is increased from 0), is shown on Fig. 8. The following conclusions can be drawn from these figures. First, $\Gamma(ka)$ is an increasing function for any value of the geometric parameter a (at least in the range $1.25 \leq a \leq 8$), so that its minimum is attained at $k = 0$, i.e. for the two-dimensional mode. So, the mode that becomes unstable first when γ increases from 0 is two-dimensional. Second, one can see that, for small to moderate values of ka ($ka \lesssim 10$), both the critical value of γ and the azimuthal wave number of the most unstable mode depend on a: both decrease when a is increased and seem to tend to a limit for large a. Third, for any fixed a and for sufficiently large ka, $\Gamma(ka)$ becomes close to a linear function whose slope is close to 2.4671. The slope is the
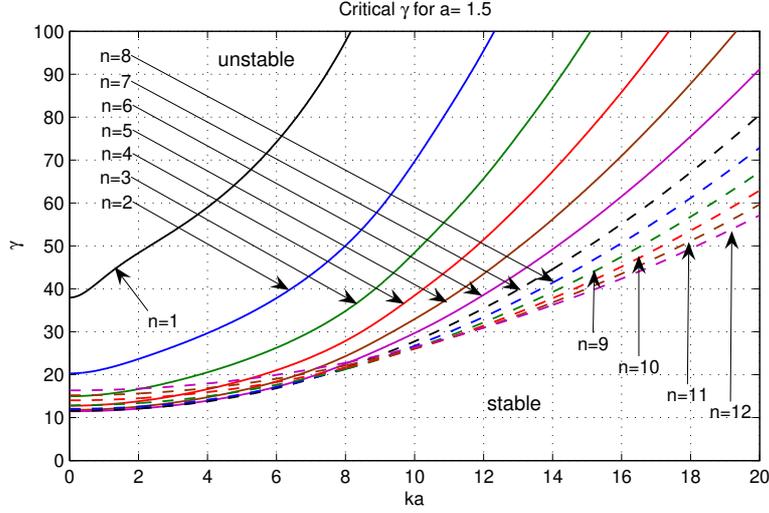
Figure 6: Neutral curves for $\beta = -1$ (converging flow), $a = 1.5$ and $n = 1, \ldots, 12$. The region above each curve is where the corresponding mode is unstable.

same as that appeared in Section 3.1.3, and this is not a coincidence: it is shown in Appendix B that the asymptotic equations ($ka \gg 1$) for the converging flow reduce to the corresponding equations for the diverging flow under a simple transformation. The comparison of Figures 2 and 7 shows that the critical values of γ for the converging flow is slightly higher than that for the diverging flow. In this sense, the converging flow is more stable than the diverging flow. Also, Fig. 8 shows that the azimuthal wave number of the most unstable mode, n, becomes independent of a and close to a linear function of ka whose slope is 1 when ka is sufficiently large (cf. Section 3.1.3).

4. Effect of viscosity

Here our aims are (i) to show that for sufficiently high Reynolds numbers the unstable inviscid modes found in the previous section give a good approximation to the corresponding viscous modes and (ii) to investigate viscous effects in the limit of high Reynolds numbers.

For the two-dimensional viscous stability problem ($k = 0$), the asymptotic behaviour of the corresponding eigenvalue problem had been studied in [2]. An asymptotic expansion of solutions of Eqs. (15)–(19) can be constructed in almost exactly the same manner and has the form

$$\sigma = \sigma_0 + R^{-1}\sigma_1 + O\left(R^{-2}\right) \tag{55}$$

and

$$\hat{u} = \hat{u}_0^r(r) + R^{-1}[\hat{u}_1^r(r) + \hat{u}_0^b(\eta)] + O\left(R^{-2}\right) \tag{56}$$

$$\hat{v} = \hat{v}_0^r(r) + \hat{v}_0^b(\eta) + R^{-1}[\hat{v}_1^r(r) + \hat{v}_1^b(\eta)] + O\left(R^{-2}\right) \tag{57}$$

$$\hat{w} = \hat{w}_0^r(r) + \hat{w}_0^b(\eta) + R^{-1}[\hat{w}_1^r(r) + \hat{w}_1^b(\eta)] + O\left(R^{-2}\right) \tag{58}$$

$$\hat{p} = \hat{p}_0^r(r) + \hat{p}_0^b(\eta) + R^{-1}[\hat{p}_1^r(r) + \hat{p}_1^b(\eta)] + O\left(R^{-2}\right) \tag{59}$$
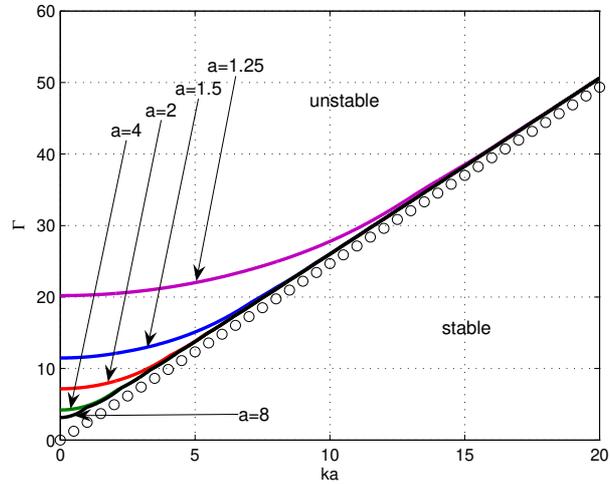
13

Figure 7: Critical γ minimized over azimuthal wave numbers $n = 1, 2, \ldots 20$ ($\Gamma = \min_n \gamma_{cr}$) for the converging flow and $a = 1.25, 1.5, 2, 4, 8$. The region above each curve is where the corresponding flow is unstable. Circles represent the asymptotic approximation to the stability boundary for large ka derived in Appendix B.
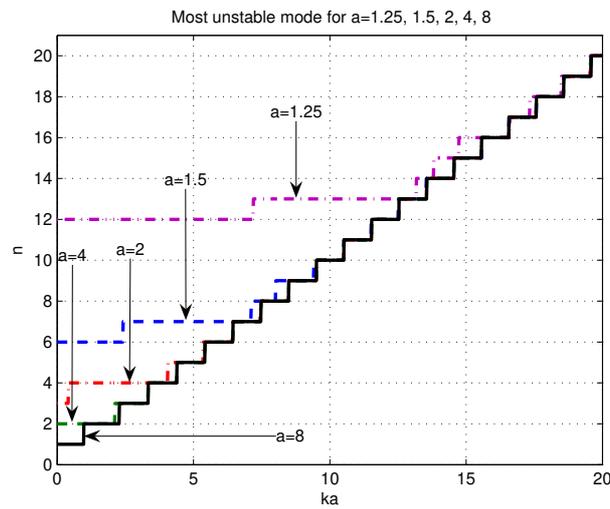

Figure 8: The azimuthal wave number of the most unstable mode, n, for the converging flow versus ka for $a = 1.25, 1.5, 2, 4, 8$.
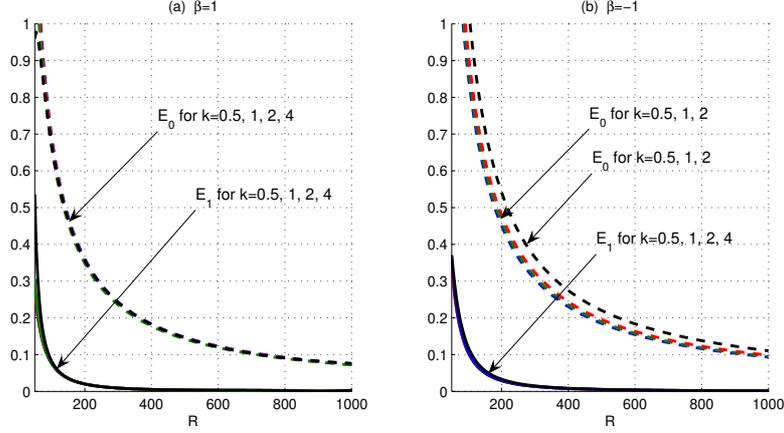
14

Figure 9: $E_0 \equiv |\sigma - \sigma_0|$ and $E_1 \equiv |\sigma - \sigma_0 - \sigma_1/R|$ versus R for $a = 2$, $n = 1$ and $k = 0.5, 1, 2$ and 4. (a) - the diverging flow with $\gamma_1 = 20$, $\gamma_2 = 0$; (b) - the converging flow with $\gamma_1 = 0$, $\gamma_2 = 20$.

for the diverging flow ($\beta = 1$) and

$$\hat{u} = \hat{u}_0^r(r) + R^{-1}[\hat{u}_1^r(r) + \hat{u}_0^b(\xi)] + O\left(R^{-2}\right) \tag{60}$$

$$\hat{v} = \hat{v}_0^r(r) + \hat{v}_0^b(\xi) + R^{-1}[\hat{v}_1^r(r) + \hat{v}_1^b(\xi)] + O\left(R^{-2}\right) \tag{61}$$

$$\hat{w} = \hat{w}_0^r(r) + \hat{w}_0^b(\xi) + R^{-1}[\hat{w}_1^r(r) + \hat{w}_1^b(\xi)] + O\left(R^{-2}\right) \tag{62}$$

$$\hat{p} = \hat{p}_0^r(r) + \hat{p}_0^b(\xi) + R^{-1}[\hat{p}_1^r(r) + \hat{p}_1^b(\xi)] + O\left(R^{-2}\right) \tag{63}$$

for the converging flow ($\beta = -1$). Here η and ξ are the boundary layer variables defined in section 2, functions with superscript "r" represent the regular part of the expansion, and functions with superscript "b" are boundary layer corrections to the regular part. The boundary layer part of the expansion exponentially decays outside the boundary layer. A brief description of the asymptotic expansion is given in Appendix C.

In Eq. (55), σ_0 is the inviscid eigenvalue discussed in the previous section, and σ_1 is the first-order viscous correction, computed in Appendix C. The exact viscous eigenvalue problem, given by Eqs. (15)–(19) was solved numerically using an adapted version of a Fourier-Chebyshev Petrov-Galerkin spectral method described by Meseguer & Trefethen [27]. We have computed the eigenvalue with largest real part, σ, numerically for a range of values of the Reynolds number R and compared the results with the inviscid eigenvalue σ_0 and the first-order viscous approximation $\sigma_0 + \sigma_1/R$. The errors of approximating σ by these are shown in Fig. 9 where $E_0 \equiv |\sigma - \sigma_0|$ and $E_1 \equiv |\sigma - \sigma_0 - \sigma_1/R|$. One can see that the dependence of E_0 and E_1 on k is very weak for both the diverging and converging flows. In fact, all curves shown in Fig. 9 are almost the same as the curve corresponding to two-dimensional perturbations shown in Fig. 2(b) of Ref. [2]. Such behaviour of the errors is typical for the above asymptotic expansion unless the axial and azimuthal wave numbers are too large.

Figures 9(a) and (b) show that even for moderate values of R such as $R = 200$ the asymptotic formula $\sigma \approx \sigma_0 + \sigma_1/R$ yields very good approximations for the eigenvalues of the viscous problem (15)–(19). This means not only that the inviscid instability studied here persists if viscosity is taken into account, but also that the asymptotic theory works well for Reynolds numbers which are not very high, and this, in turn, implies that the instability may be observed in rotating engineering and geophysical flows.

Another interesting question is whether the effect of small viscosity is stabilising or destabilising. In other words, can viscosity reduce critical values of γ? To answer this question, we computed σ_1 for critical values of γ (at which the inviscid eigenvalues σ_0 have zero real part) for various values of a and n for both the diverging and converging flows. The results are shown in Figs. 10 and 11. One can see that in all cases, $Re(\sigma_1)$ is a negative and descreasing function of k for all $k > 0$. It means that small viscosity has a stabilising effect of the flow: it makes critical values of
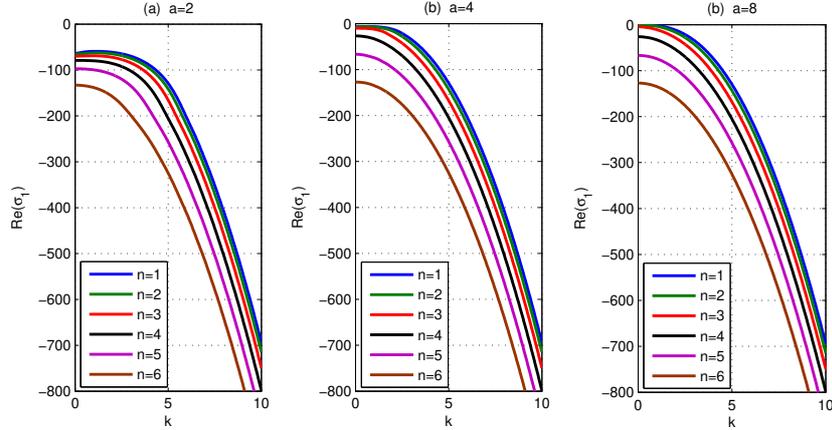
15

Figure 10: σ_1 versus k for the diverging flow ($\beta = 1$) for $n = 1, \ldots, 6$: (a) - $a = 2$; (b) - $a = 4$; (c) - $a = 8$. In each figure, curves counted from top to bottom correspond to $n = 1, 2, 3, 4, 5, 6$, respectively.

γ bigger, and this is true for both the diverging and converging flows. Figures 10 and 11 also show that the minimum stabilisation occurs for $k = 0$, i.e. for two-dimensional modes, which is a natural thing as a stronger damping of modes with higher k by viscosity should be expected. The fact that viscosity has a stabilising effect (at least at high Reynolds numbers) suggests that the instability considered in the present paper has an inviscid mechanism.

5. Discussion

We have shown that, in the limit of high radial Reynolds numbers, the linear stability problem for steady rotationally and translationally (in the z direction) invariant viscous flows between rotating porous cylinders reduces to the inviscid stability problem for a simple irrotational flow. This inviscid flow can be unstable to small three-dimensional perturbations. We gave a rigorous proof of the facts that the purely radial diverging and converging flows are stable and that unstable modes cannot be axisymmetric. Numerical calculations demonstrated that (i) for all values of the geometric parameter a in the range from 1.25 to 8, the most unstable mode (i.e. the mode that becomes unstable first when the inlet circulation, γ, is increased from 0) is two-dimensional and (ii) the critical value of γ minimized over all azimuthal modes is a strictly increasing function of the axial wave number. Note also that the only condition for the flow to be unstable is that the inlet circulation is sufficiently large irrespective of what happens at the flow outlet. Therefore, the instability can occur far beyond the Rayleigh line (that separates inertially stable and unstable regimes in the classical Couette-Taylor flow).

We have also computed the first-order viscous correction to inviscid eigenvalues and compared the asymptotic results with numerically obtained viscous eigenvalues. This demonstrated that the asymptotic results give a very good approximation even for Reynolds numbers that are not particularly high, such as $R = 200$, which suggests that the instability may be be observed in rotating engineering and geophysical flows. We have also found that, in all cases, the principal viscous corrections evaluated at the critical curves of the inviscid problem have negative real parts. This means that the small viscosity always has a stabilising effect on the flow and, therefore, the instability has an inviscid mechanism. Of course, depending on the values of the flow parameters, there may be other instabilities. For example, as was discussed in [2], the viscous boundary layers that appear near the outflow part of the boundary can also be unstable. In particular, it was shown that, at high radial Reynolds numbers, this instability is equivalent to the instability of the asymptotic suction profile (see, e.g., [28, 29, 30]). However, the viscous boundary layer instability is well separated from the instability discussed in the present paper: the former requires very large values of $|\gamma_1 - \gamma_2|$ ($|\gamma_1 - \gamma_2| > 5 \cdot 10^4$), while the latter occurs at moderate values of γ_1 and γ_2.

It is known that a purely azimuthal inviscid flow with the velocity inversely proportional to r is stable to three-dimensional perturbations (this follows from a sufficient condition for stability given by Howard & Gupta [31]). The
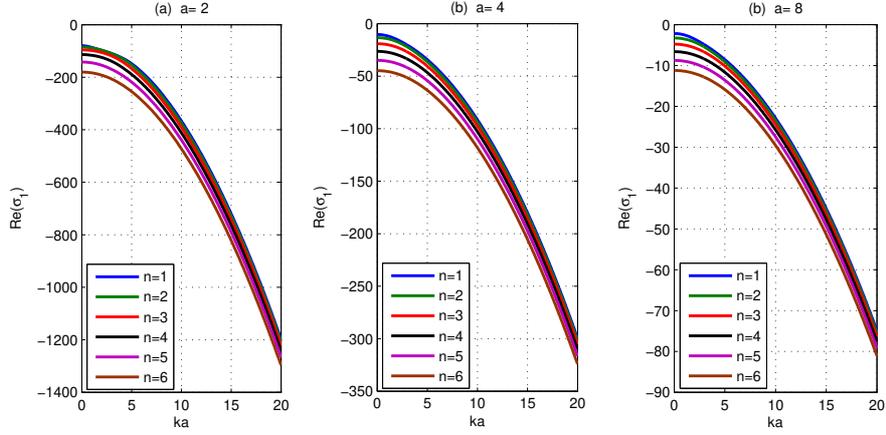
Figure 11: σ_1 versus ka for the converging flow ($\beta = -1$) for $n = 1, \ldots, 6$: (a) - $a = 2$; (b) - $a = 4$; (c) - $a = 8$. In each figure, curves counted from top to bottom correspond to $n = 1, 2, 3, 4, 5, 6$, respectively.

present paper shows that a purely radial flow is also stable to three-dimensional perturbations. These facts indicate that the physical mechanism of the instability must rely on some destabilising effect arising from the presence of both the radial and azimuthal components of the basic flow. It has been shown in our previous paper [1] that if a small radial component is added to the purely azimuthal flow, it immediately becomes unstable for any value of the ratio of the radii of the cylinders, and the growth rate is proportional to the square root of the ratio of the radial component of the velocity to the azimuthal one. The asymptotic behaviour of two-dimensional unstable eigenmodes in the limit of weak radial flow (see [1]) shows that this limit is a singular limit of the linear stability problem. Adding a weak radial flow to a purely azimuthal one results in formation of an *inviscid* boundary layer near the inflow part of the boundary, and the unstable eigenmodes are concentrated within this boundary layer. These facts suggest the following physical mechanism of the instability: in a purely azimuthal flow there are no unstable eigenmodes, but when we add a weak radial flow, this leads to appearance of new unstable eigenmodes (which do not exist at all if there is no radial flow) concentrated within a thin inviscid boundary layer near the inflow part of the boundary. This mechanism bears some resemblance to the tearing instability in the magnetohydrodynamics, where the unstable tearing mode appears when a small resistivity is taken into consideration (see Ref. [32]).

The instability considered here is oscillatory. The two-dimensional neutral modes represent azimuthal travelling waves, while the three-dimensional ones are helical waves. An oscillatory instability and appearance of azimuthal and helical waves are also present in the Couette-Taylor flow between impermeable cylinders. In the Couette-Taylor flow, these waves are observed at moderate azimuthal Reynolds numbers and are associated with viscous effects (see, e.g., [33]). The results of the present paper show that, in the presence of a radial flow, azimuthal and helical waves may appear at arbitrarily large radial Reynolds numbers, which means that the radial flow can also lead to generation of these waves. This has a certain similarity with self-oscillations observed in numerical simulations of inviscid flows through a channel of finite length [34]. Also, as was noted in [12], there are similarities between the unstable modes found here and unstable modes of the stratorotational instability (see, e.g., [13]): the latter modes are also three-dimensional waves propagating in both azimuthal and axial directions, and they persist beyond the Rayleigh line.

A more detailed analysis of the effect of the radial flow on the stability of the basic viscous flow (6) at low and moderate radial Reynolds numbers requires a further investigation which would take full account of the viscosity. A particularly interesting question that arises in this context is the relation between the instability studied here and the classical centrifugal instability that leads to the formation of the Taylor vortices. Here is an interesting paradox: in the inviscid theory, axisymmetric modes cannot be unstable, but it is well known that the monotonic instability with respect to axisymmetric perturbation occurs in the Couette-Taylor flow with radial flow (see, e.g., [5, 8]). Our hypothesis is that the monotonic axisymmetric and oscillatory non-axisymmetric instabilities are well separated in the

space of parameters of the problem. If this were so, it would mean that our instability can be observed experimentally. This, however, requires a further theoretical study and is a topic of a continuing investigation.

The results presented here are mainly of theoretical interest. However, as was argued by Gallet et al [11], they may be relevant to astrophysical flows such as accretion discs (see also Refs. [12, 35]). Our results may also shed some light on the physical mechanism of the formation of strong rotating jets in flows produced by a rotating disk which had been observed experimentally (see [36, 37]).

Acknowledgements

Appendix A.

Here we will show that, for the diverging flow, (i) there are no unstable modes if the basic flow is purely radial and (ii) all axisymmetric modes are stable. To do this, we employ the following theorem of Pólya (problem 177 of Part V in [25], see also [26]).

Pólya's theorem. *Let the function $f(t)$ be continuously differentiable and positive for $0 < t < 1$, and also let $\int_0^1 f(t)dt$ exist. The entire function defined by the integral*

$$\int_0^1 f(t)e^{zt}dt = F(z)$$

has no zeros

$$\text{in the half-plane} \quad Re\, z \geq 0, \quad \text{if} \quad f'(t) > 0,$$
$$\text{in the half-plane} \quad Re\, z \leq 0, \quad \text{if} \quad f'(t) < 0.$$

It should be noted that the interval $(0, 1)$ in the above theorem can be replaced by an arbitrary finite interval (a, b).

Consider first the case of purely radial flow. For $\gamma = 0$, the dispersion relation (49) can be written as

$$D(\sigma) = \frac{1}{a} \int_1^a e^{-\sigma \frac{r^2}{2}} \Phi(kr)\, r\, dr \tag{A.1}$$

where

$$\Phi(s) = sI'_n(s)s_0K'_n(s_0) - s_0I'_n(s_0)sK'_n(s), \quad s_0 \equiv ka. \tag{A.2}$$

The change of variable of integration, $\xi = r^2/2$, transforms (A.1) to

$$D(\sigma) = \frac{1}{a} \int_{1/2}^{a^2/2} e^{-\sigma\xi} f(\xi)\, d\xi, \quad f(\xi) \equiv \Phi(k\sqrt{2\xi}). \tag{A.3}$$

If function $f(\xi)$ were such that $f(\xi) > 0$ and $f'(\xi) < 0$ for $\xi \in \left(\frac{1}{2}, \frac{a^2}{2}\right)$, then the above theorem implies that $D(\sigma)$ has no zeros in the half-plane $Re\, \sigma \geq 0$, i.e. all its zeros satisfy $Re\, \sigma < 0$, which means that all modes are stable.

The conditions for function $f(\xi)$ that should be checked are equivalent to the following conditions for $\Phi(s)$:

$$\Phi(s) > 0 \quad \text{and} \quad \Phi'(s) < 0 \quad \text{for} \quad s \in (k, s_0). \tag{A.4}$$

It is convenient to introduce function $\Psi(s)$ by the formula

$$\Psi(s) = I_n(s)s_0K'_n(s_0) - s_0I'_n(s_0)K_n(s). \tag{A.5}$$

18

Conditions (A.4), expressed in terms of $\Psi(s)$, become

$$s\Psi'(s) > 0 \quad \text{for} \ \ s \in (k, s_0), \tag{A.6}$$

$$(s\Psi')'(s) < 0 \quad \text{for} \ \ s \in (k, s_0). \tag{A.7}$$

It is easy to see that function $\Psi(s)$ is a solution of the modified Bessel differential equation

$$\frac{1}{s} \frac{d}{ds} \left(s \frac{d\Psi}{ds} \right) - \left(1 + \frac{n^2}{s^2} \right) \Psi = 0 \tag{A.8}$$

and satisfies the following boundary conditions:

$$\Psi(s_0) = -1 \quad \text{and} \quad \Psi'(s_0) = 0, \tag{A.9}$$

where the first of these conditions follows from the Wronskian relation (47).

First we prove the following auxiliary statement: $\Psi(s) \neq 0$ and $\Psi'(s) \neq 0$ for all $k \leq s < s_0$. To do this, we assume that either $\Psi(s_*) = 0$ or $\Psi'(s_*) = 0$ for some $s_* \in [k, s_0)$. Multiplying Eq. (A.8) by $s \Psi(s)$ and integrating from s_* to s_0, we find that

$$\int_{s_*}^{s_0} \left(1 + \frac{n^2}{s^2} \right) \Psi^2(s) s \, ds \ = \ \int_{s_*}^{s_0} \Psi(s) \left(s \Psi' \right)'(s) \, ds$$

$$= \ s \Psi(s) \Psi'(s) \Big|_{s_*}^{s_0} - \int_{s_*}^{s_0} \Psi'^2(s) s \, ds.$$

Therefore, if either $\Psi(s_*) = 0$ or $\Psi'(s_*) = 0$, then

$$\int_{s_*}^{s_0} \left(1 + \frac{n^2}{s^2} \right) \Psi^2(s) s \, ds = - \int_{s_*}^{s_0} \Psi'^2(s) s \, ds,$$

which is impossible. Therefore, both $\Psi(s)$ and $\Psi'(s)$ must be nonzero for all $k \leq s < s_0$.

Now we are ready to prove the required properties of $\Psi(s)$. Since $\Psi(s_0) < 0$ and $\Psi(s)$ cannot change sign for $s \in [k, s_0)$, we conclude that $\Psi(s) < 0$ for all $s \in [k, s_0)$. Then, in view of the differential equation (A.8), we obtain

$$(s \Psi')'(s) = s \left(1 + \frac{n^2}{s^2} \right) \Psi(s) \quad \Rightarrow \quad (s \Psi')'(s) < 0.$$

We have thus proved (A.7). To prove (A.6), we observe that it follows from the differential equation (A.8) and the boundary conditions that $\Psi''(s_0) < 0$. This means that $\Psi'(s) > \Psi'(s_0) = 0$ at least near the end point $s = s_0$. But since $\Psi'(s)$ cannot change sign, it must be positive for all $s \in [k, s_0)$, so that condition (A.6) is satisfied.

Thus, the Pólya theorem implies that for the purely radial converging basic flow ($\gamma = 0$), there are no unstable modes.

It is easy to see that for the axisymmetric mode ($n = 0$) and for any γ, the dispersion relation (49) also reduces to Eq. (A.3) with $n = 0$, so that we may conclude that there are no growing axisymmetric modes.

Appendix B.

Here we construct an asymptotic expansion of the solution to the inviscid eigenvalue problem (20)–(22), (18) and (23) or (24) for large axial wave number $k \gg 1$. It is convenient to rewrite this problem in a form different from what has been obtained in Section 3.1.1.

Let $H(r) = r\hat{u}(r)$. Then Eq. (36) can be written as

$$\frac{in}{r} H'(r) - \left(k^2 + \frac{n^2}{r^2} \right) G(r) = 0 \tag{B.1}$$

19

where $G = r\hat{v}(r)$. It follows from (B.1) that $\hat{\omega}_3(r)$, given by Eq. (28), can be rewritten in term of H only as

$$\hat{\omega}_3 = \frac{in}{r} \partial_r \left(\frac{r}{n^2 + k^2 r^2} H'(r) \right) - \frac{in}{r^2} H(r).$$

Substituting this into Eq. (31) and dropping the inessential factor in yields the equation

$$\left(\sigma + \frac{in\gamma}{r^2} + \frac{\beta}{r} \partial_r \right) \left[\frac{1}{r} \partial_r \left(\frac{r}{n^2 + k^2 r^2} H'(r) \right) - \frac{1}{r^2} H(r) \right] = 0. \tag{B.2}$$

Equation (B.2) must be solved subject to boundary conditions (23) or (24) which, in terms of H, can be written as

$$H(1) = 0, \quad H(a) = 0 \tag{B.3}$$

and either

$$H'(1) = 0 \tag{B.4}$$

for the diverging flow ($\beta = 1$) or

$$H'(a) = 0 \tag{B.5}$$

for the converging flow ($\beta = -1$). Equations (B.4) and (B.5) follow from the incompressibility condition (18).

Diverging flow. Figure 3 indicates that the azimuthal number of the most unstable mode behaves like $n \sim k$ for large k. Therefore, in order to capture the stability boundary for large k, we consider the limit

$$k \to \infty, \quad n \to \infty, \quad n \sim k.$$

So, we set $n = \alpha k$ in Eq. (B.2) where $\alpha > 0$ and does not depend on k. We also assume that

$$\gamma = \tilde{\gamma} k \quad \text{and} \quad \sigma = -i\tilde{\gamma}\alpha k^2 + \tilde{\sigma} k \tag{B.6}$$

where $\tilde{\gamma} = O(1)$ and $\tilde{\sigma} = O(1)$ as $k \to \infty$. Incorporating these assumptions into Eq. (B.2), we get

$$\left[i\tilde{\gamma}\alpha \left(\frac{1}{r^2} - 1 \right) + \tilde{\sigma} \frac{1}{k} + \frac{1}{k^2} \frac{1}{r} \partial_r \right] \left[\frac{1}{k^2} \frac{1}{r} \partial_r \left(\frac{r}{\alpha^2 + r^2} H'(r) \right) - \frac{1}{r^2} H(r) \right] = 0. \tag{B.7}$$

In the limit $k \to \infty$, this equation reduces to

$$-i\tilde{\gamma}\alpha \left(\frac{1}{r^2} - 1 \right) \frac{H}{r^2} = 0.$$

This implies that $H(r)$ must be zero everywhere except a thin boundary layer near $r = 1$ where the above leading order term becomes small ($O(k^{-1})$ as $k \to \infty$) and of the same order as some terms which we have discarded. To treat this boundary layer, we introduce the boundary layer variable ξ such that

$$r = 1 + \frac{1}{k} \xi$$

and rewrite Eq. (B.7) in terms of ξ. At leading order, we obtain

$$\left[\tilde{\sigma} - 2i\tilde{\gamma}\alpha\xi + \partial_\xi \right] \left[\frac{1}{1 + \alpha^2} H''(\xi) - H(\xi) \right] = 0. \tag{B.8}$$

Boundary conditions (B.3), (B.4), written in terms of ξ, take the form

$$H(0) = 0, \quad H'(0) = 0, \quad H \to 0 \text{ as } \xi \to \infty. \tag{B.9}$$
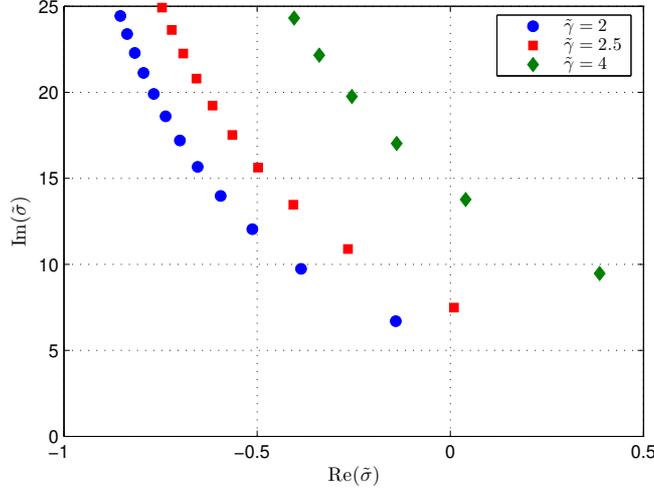
20

Figure B.12: Roots of Eq. (B.12) for $\alpha = 1$ and $\tilde{\gamma} = 2, 2.5, 4$.

The solution of Eq. (B.8), satisfying the first and the last of conditions (B.9), can be written as

$$H(\xi) = \frac{C_1}{2\sqrt{2}} \int\limits_0^\infty e^{-\tilde{\sigma}s + i\tilde{\gamma}\alpha s^2} \left[e^{-\mu(\alpha)|\xi+s|} - e^{-\mu(\alpha)|\xi-s|} \right] ds \tag{B.10}$$

where $\mu(\alpha) = \sqrt{1 + \alpha^2}$ and C_1 is an arbitrary constant. Note that formula (B.10) is valid only for $\tilde{\sigma}$ satisfying the condition $\mathrm{Re}(\tilde{\sigma}) > 0$. This means that our asymptotic result can only describe unstable eigenmodes.

Substituting (B.10) into the second boundary condition (B.9), we find that the condition of existence of non-trivial solutions of problem (B.8), (B.9) is

$$D_2(\tilde{\sigma}, \tilde{\gamma}, \alpha) \equiv \int\limits_0^\infty e^{-\tilde{\sigma}s + i\tilde{\gamma}\alpha s^2} e^{-\mu(\alpha)s} ds = 0. \tag{B.11}$$

Equation (B.11) represents the dispersion relation for eigenvalues $\tilde{\sigma}$. Note that $D_2(\tilde{\sigma}, \tilde{\gamma}, \alpha)$, given by this formula, makes sense for $\tilde{\sigma}$ such that $\mathrm{Re}(\tilde{\sigma}) > -\mu(\alpha)$ and may have zeroes with $-\mu(\alpha) < \mathrm{Re}(\tilde{\sigma}) \leq 0$. However, only zeros of $D_2(\tilde{\sigma}, \tilde{\gamma}, \alpha)$ with $\mathrm{Re}(\tilde{\sigma}) > 0$ represent asymptotic approximations to the eigenvalues of the original problem.

To make calculations easier, it is convenient to transform the dispersion relation to an equivalent form by deforming the path of integration on the complex plane of variables s from the positive real axis to the half-line: $s = r e^{i\pi/4}$, $r \in [0, \infty)$. Then the dispersion relation takes the form

$$\int\limits_0^\infty e^{-\tilde{\gamma}\alpha r^2 - e^{i\pi/4}[\tilde{\sigma} + \mu(\alpha)] r} dr = 0. \tag{B.12}$$

This equation can be further rewritten in term of the error function $\mathrm{erf}(z)$, but we do not do this here as Eq. (B.12) is more convenient for numerical calculations. Typical roots of Eq. (B.12) are shown in Fig. B.12. Evidently, when $\tilde{\gamma}(\alpha)$ is smaller than some critical value $\tilde{\gamma}_{cr}(\alpha)$, all roots are in the left half plane, and when $\tilde{\gamma}(\alpha) > \tilde{\gamma}_{cr}(\alpha)$, there is at least one root with $\mathrm{Re}(\tilde{\sigma}) > 0$, which represents an asymptotic approximation of an unstable eigenvalue in the original problem.

21

To determine $\tilde{\gamma}_{cr}(\alpha)$ and $\lambda_{cr}(\alpha)$, we require $\tilde{\sigma}$ to be purely imaginary, i.e. $\tilde{\sigma} = i\lambda$ with $\lambda \in \mathbb{R}$. The dispersion relation (B.12) becomes

$$\int_0^\infty e^{-\tilde{\gamma}\alpha\, r^2 - e^{i\pi/4}[i\lambda + \mu(\alpha)]\, r}\, dr = 0. \tag{B.13}$$

Equation (B.13) has many roots. These roots corresponds to values of $\tilde{\gamma}(\alpha)$ at which one of the zeros of the function $D_2(\tilde{\sigma}, \tilde{\gamma}, \alpha)$ crosses the imaginary axis on the complex $\tilde{\sigma}$-plane. We are only interested in the root that corresponds to the smallest value of $\tilde{\gamma}$ because it is this root that determines the stability boundary. In what follows we will consider only this root of Eq. (B.13).

It turns out (the proof is below) that the function $\tilde{\gamma}_{cr}(\alpha)$ has a local minimum at $\alpha = 1$ (i.e. when $n = k$ as $k \to \infty$). Calculations yield

$$\min_\alpha \tilde{\gamma}_{cr}(\alpha) = \tilde{\gamma}_{cr}(1) \approx 2.4671 \quad \text{and} \quad \lambda_{cr}(1) \approx 7.4331.$$

Since we are interested in the asymptotic behaviour of the stability boundary on the (k, γ), we choose $\alpha = 1$ corresponding to the minimum value of $\tilde{\gamma}_{cr}(\alpha)$. Thus, the behaviour of the stability boundary in the limit $k \to \infty$ is given by

$$\min_\alpha \gamma_{cr}(\alpha, k) = 2.4671\, k + O(1).$$

This is shown by circles in Fig. 2.

To prove that $\tilde{\gamma}_{cr}(\alpha)$ attains its minimum value at $\alpha = 1$, we change the variable of integration in Eq. (B.13): $r = \zeta \sqrt{2}/\mu(\alpha)$. This transforms (B.13) to the equation

$$\frac{\sqrt{2}}{\mu(\alpha)} \int_0^\infty e^{-\gamma_*\zeta^2 - e^{i\pi/4}[i\lambda_* + \sqrt{2}]\zeta}\, d\zeta = 0 \tag{B.14}$$

where

$$\gamma_* = \frac{2\alpha}{\mu^2(\alpha)}\, \tilde{\gamma}, \quad \lambda_* = \frac{\sqrt{2}}{\mu(\alpha)}\, \lambda.$$

Then we make an observation that, up to an inessential constant factor, Eq. (B.14) is exactly the same as Eq. (B.13) for $\alpha = 1$, with $\tilde{\gamma}$ and λ replaced by γ_* and λ_*. This implies that, if γ_* and λ_* represent a root of Eq. (B.14), then $\gamma_* = \tilde{\gamma}_{cr}(1)$ and $\lambda_* = \lambda_{cr}(1)$. This fact and the definition of γ_* and λ_* have a consequence that

$$\tilde{\gamma}_{cr}(\alpha) = \frac{1 + \alpha^2}{2\alpha}\, \tilde{\gamma}_{cr}(1), \quad \lambda_{cr}(\alpha) = \frac{\sqrt{1 + \alpha^2}}{\sqrt{2}}\, \lambda_{cr}(1).$$

Since function $f(\alpha) = (1 + \alpha^2)/(2\alpha)$ attains its minimum value at $\alpha = 1$ and $f(1) = 1$, we obtain the required property of $\tilde{\gamma}_{cr}(\alpha)$.

Converging flow. For the converging flow, a similar analysis shows that in the limit

$$ka \to \infty, \quad n = \alpha\, ka,$$

the eigenvalue problem (B.2), (B.3), (B.5) reduces to

$$\left[\tilde{\sigma} + 2i\tilde{\gamma}\alpha\, \eta + \partial_\eta\right]\left[\frac{1}{1 + \alpha^2}\, H''(\eta) - H(\eta)\right] = 0 \tag{B.15}$$

and

$$H(0) = 0, \quad H'(0) = 0, \quad H \to 0 \text{ as } \eta \to \infty. \tag{B.16}$$

where η, $\tilde{\gamma}$ and $\tilde{\sigma}$ are defined by

$$\eta = ka\left(1 - \frac{r}{a}\right), \quad \gamma = \tilde{\gamma}\, ka, \quad \sigma = \frac{1}{a^2}\left[-i\tilde{\gamma}\alpha(ka)^2 + \tilde{\sigma}\, ka\right].$$

22

It is easy to see that, the complex conjugate of Eq. (B.15) is equivalent to Eq. (B.8), with $\tilde{\sigma}$ replaced by its complex conjugate $\overline{\tilde{\sigma}}$. This means that if $\tilde{\sigma}$ and $H(\xi)$ represent a solution of problem (B.8), (B.9), then $\overline{\tilde{\sigma}}$ and and $\overline{H}(\eta)$ solve problem (B.15), (B.16). Therefore, the asymptotic result for the converging flow can be obtained from that for the diverging flow by simply replacing $\tilde{\sigma}$ by $\overline{\tilde{\sigma}}$ and $H(\xi)$ by $\overline{H}(\eta)$. Hence, we obtain

$$\min_\alpha \tilde{\gamma}_{cr}(\alpha) = \tilde{\gamma}_{cr}(1) \approx 2.4671, \quad \lambda_{cr}(1) \approx -7.4331$$

where $\lambda_{cr} = \mathrm{Im}(\tilde{\sigma})$ when $\mathrm{Re}(\tilde{\sigma}) = 0$. This means that in the limit $ka \to \infty$, $n = \alpha\,ka$, we have

$$\min_\alpha \gamma_{cr}(\alpha, ka) = 2.4671\,ka + O(1).$$

Appendix C.

Here we derive the asymptotic approximation (55)–(63). We will do this separately for the diverging and converging flows.

Appendix C.1. Diverging flow ($\beta = 1$)

To obtain the regular part of the expansion (that is valid everywhere except the boundary layer near $r = a$), we substitute the asymptotic formula for the azimuthal velocity (9) and Eqs. (55)–(59) into (15)–(18), discard all boundary layer terms and collect terms containing equal powers of $1/R$. As a result, we obtain a sequence of equations, the first two of which can be written as

$$K\mathbf{v}_0^r = 0, \tag{C.1}$$
$$K\mathbf{v}_1^r = -\sigma_1\mathbf{v}_0^r + B\mathbf{v}_0^r. \tag{C.2}$$

Here $\mathbf{v}_k^r = (\hat{u}_k^r, \hat{v}_k^r, \hat{w}_k^r)$ for $k = 0, 1$ and operators K and B are defined as

$$K\mathbf{v}_k^r = \begin{pmatrix} \left(\frac{h_1'(r)}{r} + \frac{1}{r}\partial_r\right)\hat{u}_k^r - \frac{1}{r^2}\hat{u}_k^r - \frac{2\gamma_1}{r^2}\hat{v}_k^r + \partial_r\,\hat{p}_k^r \\ \left(\frac{h_1'(r)}{r} + \frac{1}{r}\partial_r\right)\hat{v}_k^r + \frac{1}{r^2}\hat{v}_k^r + \frac{in}{r}\,\hat{p}_k^r \\ \left(\frac{h_1'(r)}{r} + \frac{1}{r}\partial_r\right)\hat{w}_k^r + ik\,\hat{p}_k^r \end{pmatrix} \tag{C.3}$$

and

$$B\mathbf{v}_0^r = \begin{pmatrix} L\hat{u}_0^r - \frac{1}{r^2}\hat{u}_0^r - \frac{2in}{r^2}\hat{v}_0^r \\ L\hat{v}_0^r - \frac{1}{r^2}\hat{v}_0^r + \frac{2in}{r^2}\hat{u}_0^r \\ L\hat{w}_0^r \end{pmatrix}. \tag{C.4}$$

In Eq. (C.3),

$$h_1(r) = \sigma_0\frac{r^2}{2} + in\gamma_1\log r.$$

and $\hat{p}_k^r$ can be eliminated using the incompressibility condition

$$\partial_r\left(r\hat{u}_0^r\right) + in\,\hat{v}_0^r + ikr\hat{w}_0^r = 0. \tag{C.5}$$

Boundary conditions for $\mathbf{v}_0^r$ and $\mathbf{v}_1^r$ are obtained by substituting (56)–(59) into (19) and collecting terms containing equal powers of $1/R$. This yields

$$\hat{u}_0^r(1) = \hat{u}_0^r(a) = 0, \tag{C.6}$$
$$\hat{v}_0^r(1) = \hat{w}_0^r(1) = 0, \tag{C.7}$$
$$\hat{v}_0^r(a) + \hat{v}_0^b(0) = 0, \quad \hat{w}_0^r(a) + \hat{w}_0^b(0) = 0, \tag{C.8}$$
$$\hat{u}_1^r(1) = 0, \quad \hat{u}_1^r(a) + \hat{u}_0^b(0) = 0, \tag{C.9}$$
$$\hat{v}_1^r(1) = \hat{w}_1^r(1) = 0. \tag{C.10}$$

23

We did not present boundary conditions for $\hat{v}_1^r$ and $\hat{w}_1^r$ at $r = a$, as they are not needed in what follows.

Equation (C.1) and boundary conditions (C.6) and (C.7) represent the inviscid eigenvalue problem considered in Section 3. After the insivcid problem is solved, σ_0 and $\mathbf{v}_0^r$ are known. Then boundary conditions (C.8) are employed to find the boundary layer corrections $\hat{v}_0^b$ and $\hat{w}_0^b$. After that, the boundary layer part of the radial component of the velocity, $\hat{u}_0^b$, can be found from the incompressibility condition. Once, $\hat{u}_0^b$ is known, Eqs. (C.9) and (C.10) give us boundary conditions for Eq. (C.2), which can then be solved, and the entire procedure can repeated as many times as necessary yielding higher order approximations. However, to find σ_1, we do not need to calculate the solution of (C.2) explicitly, all we need is to ensure that a solution does exist. Before describing how this can be done, we need to say a few words about the boundary layer.

The boundary layer approximations are obtained as follows. We substitute the asymptotic formula Eq. (9) and Eqs. (55)–(59) into (15)–(18) and take into account that the regular part satisfies Eqs. (C.1) and (C.2). Then we make the change of variable $r = a(1 - R^{-1}\eta)$, expand every function of $a(1 - R^{-1}\eta)$ in Taylor's series at $R^{-1} = 0$ and, finally, collect terms of the equal powers of R^{-1}. At leading order, the boundary layer equations are given by

$$\partial_\eta^2 \hat{v}_0^b + \partial_\eta \hat{v}_0^b = 0, \tag{C.11}$$

$$\partial_\eta^2 \hat{w}_0^b + \partial_\eta \hat{w}_0^b = 0, \tag{C.12}$$

$$-\partial_\eta \hat{u}_0^b + in\hat{v}_0^b + ika\hat{w}_0^b = 0. \tag{C.13}$$

The solutions of Eqs. (C.11)–(C.13) that satisfy boundary conditions (C.8) and the condition of decay at infinity are

$$\hat{v}_0^b = -\hat{v}_0^r(a)\, e^{-\eta}, \quad \hat{w}_0^b = -\hat{w}_0^r(a)\, e^{-\eta}, \quad \hat{u}_0^b = -\int_\eta^\infty \left(in\hat{v}_0^b(s) + ika\hat{w}_0^b(s)\right) ds.$$

Here the constant of integration has been chosen so as to guarantee that $\hat{u}_0^b(\eta)$ decays at infinity. Hence, the boundary condition for $\hat{u}_1^r(r)$ at $r = a$ can be written as

$$\hat{u}_1^r(a) = -\hat{u}_0^b(0) = -in\hat{v}_0^r(a) - ika\hat{w}_0^r(a). \tag{C.14}$$

Now consider the non-homogeneous equation (C.2). It has a solution only if its right hand side satisfies a certain solvability condition. To formulate it, we define the inner product

$$\langle \mathbf{g}, \mathbf{f} \rangle = \int_1^a \overline{\mathbf{g}} \cdot \mathbf{f}\, r\, dr = \int_1^a \left(\overline{g}_1 f_1 + \overline{g}_2 f_2 + \overline{g}_3 f_3\right) r\, dr$$

where $\mathbf{g} = (g_1, g_2, g_3)$, $\mathbf{f} = (f_1, f_2, f_3)$, and $\overline{\mathbf{g}}$ is the complex conjugate of $\mathbf{g}$. With respect to this inner product, we define the adjoint operator $\mathbf{g} \mapsto K^*\mathbf{g}$ by

$$\langle \mathbf{g}, K\mathbf{f} \rangle = \langle K^*\mathbf{g}, \mathbf{f} \rangle$$

for any functions $\mathbf{f}$ and $\mathbf{g}$ satisfying the incompressibility conditions

$$\partial_r (rf_1) + in f_2 + ikrf_3 = 0, \quad \partial_r (rg_1) + in g_2 + ikrg_3 = 0$$

and the boundary conditions

$$f_1(1) = f_2(1) = f_3(1) = 0, \quad f_1(a) = 0, \tag{C.15}$$

$$g_1(1) = 0, \quad g_1(a) = g_2(a) = g_3(a) = 0. \tag{C.16}$$

Note that the boundary conditions for $\mathbf{f}$ and $\mathbf{g}$ are different.

Now let $\mathbf{g}$ satisfy boundary conditions (C.16) and be a solution of the equation

$$K^*\mathbf{g} = \begin{pmatrix} \left(\frac{\bar{h}_1'(r)}{r} - \frac{1}{r}\partial_r\right)g_1 - \frac{1}{r^2}g_1 + \partial_r \alpha \\ \left(\frac{\bar{h}_1'(r)}{r} - \frac{1}{r}\partial_r\right)g_2 + \frac{1}{r^2}g_2 - \frac{2\gamma_1}{r^2}g_1 + \frac{in}{r}\alpha \\ \left(\frac{\bar{h}_1'(r)}{r} - \frac{1}{r}\partial_r\right)g_3 + ik\,\alpha \end{pmatrix} = 0$$

24

where function α can be eliminated using the incompressibility condition for $\mathbf{g}$. Taking inner product of Eq. (C.2) with $\mathbf{g}$ gives us the required solvability condition:

$$Q_1 = -\sigma_1 Q_2 + Q_3$$

where

$$Q_1 = \langle \mathbf{g}, K\mathbf{v}_1^r \rangle, \quad Q_2 = \langle \mathbf{g}, \mathbf{v}_0^r \rangle, \quad Q_3 = \langle \mathbf{g}, B\mathbf{v}_0^r \rangle.$$

Hence,

$$\sigma_1 = \frac{Q_3 - Q_1}{Q_2}. \tag{C.17}$$

Below are the explicit formulae for Q_1, Q_2 and Q_3 that can be obtained after lengthy but standard calculations:

$$Q_1 = \left(n^2 + k^2 a^2\right) \int_1^a e^{-h_1(r)} \Theta(kr) \, r dr,$$

$$Q_2 = -\frac{1}{2} \int_1^a e^{-h_1(r)} \Phi(kr) \, r^3 dr,$$

$$Q_3 = \left\{ \int_1^a e^{-h_1(r)} W(r) \Phi(kr) \, r dr + k^2 \int_1^a e^{-h_1(r)} \left(r^2 - 1\right) \Psi(kr) \, r dr \right\},$$

where functions $\Phi(s)$ and $\Psi(s)$ are defined in Appendix A and

$$\Theta(s) = I_n(s_0) s K_n'(s) - s I_n'(s) K_n(s_0) \quad (s_0 = ka),$$
$$W(r) = -\sigma_0^2 \frac{r^4}{4} + \left(\frac{k^2}{2} + \sigma_0(1 - in\gamma_1)\right) r^2 + n^2 \left(1 + \gamma_1^2\right) \log r.$$

Appendix C.2. Converging flow ($\beta = -1$)

Similar analysis leads to the inviscid problem problem for the converging flow

$$M\mathbf{v}_0^r = 0, \tag{C.18}$$

where

$$M\mathbf{v}_k^r = \begin{pmatrix} \left(\frac{h_2'(r)}{r} - \frac{1}{r}\partial_r\right)\hat{u}_k^r - \frac{1}{r^2}\hat{u}_k^r - \frac{2\gamma_1}{r^2}\hat{v}_k^r + \partial_r \hat{p}_k^r \\ \left(\frac{h_2'(r)}{r} - \frac{1}{r}\partial_r\right)\hat{v}_k^r + \frac{1}{r^2}\hat{v}_k^r + \frac{in}{r}\hat{p}_k^r \\ \left(\frac{h_2'(r)}{r} - \frac{1}{r}\partial_r\right)\hat{w}_k^r + ik\,\hat{p}_k^r \end{pmatrix} \tag{C.19}$$

where $h_2(r) = \sigma_0 r^2/2 + in\gamma_2 \log r$.

Let $\mathbf{q}$ be a solution of the equation

$$M^*\mathbf{q} = \begin{pmatrix} \left(\frac{\bar{h}_2'(r)}{r} + \frac{1}{r}\partial_r\right)q_1 - \frac{1}{r^2}q_1 + \partial_r \alpha \\ \left(\frac{\bar{h}_2'(r)}{r} + \frac{1}{r}\partial_r\right)q_2 + \frac{1}{r^2}q_2 - \frac{2\gamma_1}{r^2}q_1 + \frac{in}{r}\alpha \\ \left(\frac{\bar{h}_2'(r)}{r} + \frac{1}{r}\partial_r\right)q_3 + ik\,\alpha \end{pmatrix} = 0, \tag{C.20}$$

satisfying the incompressibility condition and the boundary conditions

$$q_1(1) = q_2(1) = q_3(1) = 0, \quad q_1(a) = 0 \tag{C.21}$$

In Eq. (C.20), α can be eliminated using the incompressibility condition for $\mathbf{q}$. Then the first viscous correction to the inviscid eigenvalues is given by

$$\sigma_1 = \frac{P_3 - P_1}{P_2}. \tag{C.22}$$

where

$$P_1 = \langle \mathbf{q}, M\mathbf{v}_1^r \rangle, \quad P_2 = \langle \mathbf{q}, \mathbf{v}_0^r \rangle, \quad P_3 = \langle \mathbf{q}, B\mathbf{v}_0^r \rangle.$$

with operator B defined by Eq. (C.4). The explicit formulae for P_1, P_2 and P_3 can be obtained after simple but lengthy calculations and are given by

$$P_1 = -\left(n^2 + k^2\right) \int_1^a e^{h_2(r)} \tilde{\Theta}(r)\, r dr,$$

$$P_2 = \frac{1}{2} \int_1^a e^{h_2(r)} \tilde{\Phi}(r)\, r^3 dr,$$

$$P_3 = \left\{ \int_1^a e^{h_2(r)} \tilde{W}(r) \tilde{\Phi}(r)\, r dr + k^2 \int_1^a e^{h_2(r)} \left(a^2 - r^2\right) Q(r)\, r dr \right\},$$

where

$$\tilde{\Theta}(r) = I_n(k)\, kr\, K_n'(kr) - kr\, I_n'(kr)\, K_n(k),$$
$$\tilde{\Phi}(r) = kr\, I_n'(kr)\, k\, K_n'(k) - k\, I_n'(k)\, kr\, K_n'(kr),$$
$$\tilde{W}(r) = \sigma_0^2 \frac{r^4}{4} - \left(\frac{k^2}{2} - \sigma_0(1 + in\gamma_2)\right) r^2 - n^2 \left(1 + \gamma_2^2\right) \log r,$$
$$Q(r) = I_n(kr)\, k\, K_n'(k) - k\, I_n'(k)\, K_n(kr).$$

[1] K. Ilin, A. Morgulis, Instability of an inviscid flow between porous cylinders with radial flow. *J. Fluid Mech.* **730** (2013) 364–378.
[2] K. Ilin, A. Morgulis, Instability of a two-dimensional viscous flow in an annulus with permeable walls to two-dimensional perturbations. *Phys. Fluids* **27** (2015) 044107.
[3] S. K. Bahl, Stability of viscous flow between two concentric rotating porous cylinders. *Def. Sci. J.* **20**(3) (1970) 89–96.
[4] S. Chang, W. K. Sartory, Hydromagnetic stability of dissipative flow between rotating permeable cylinders. *J. Fluid Mech.* **27** (1967) 65–79.
[5] K. Min, R. M. Lueptow, Hydrodynamic stability of viscous flow between rotating porous cylinders with radial flow. *Phys. Fluids* **6** (1994) 144–151.
[6] A. A. Kolyshkin, R. Vaillancourt, Convective instability boundary of Couette flow between rotating porous cylinders with axial and radial flows. *Phys. Fluids* **9** (1997) 910–918.
[7] V. Kolesov, L. Shapakidze, On oscillatory modes in viscous incompressible liquid flows between two counter-rotating permeable cylinders. In: *Trends in Applications of Mathematics to Mechanics* (ed. G. Iooss, O. Gues & A Nouri), Chapman and Hall/CRC (1999), pp. 221–227.
[8] E. Serre, M. A. Sprague, R. M. Lueptow, Stability of Taylor-Couette flow in a finite-length cavity with radial throughflow. *Phys. Fluids* **20**(3) (2008) 034106.
[9] D. Martinand, E. Serre, R. M. Lueptow, Absolute and convective instability of cylindrical Couette flow with axial and radial flows. *Phys. Fluids* **21**(10) (2009) 104102.
[10] H. Fujita, H. Morimoto, H. Okamoto, Stability analysis of NavierStokes flows in annuli. *Mathematical methods in the applied sciences* **20**(11) (1997) 959–978.
[11] B. Gallet, C. R. Doering, E. A. Spiegel, Destabilizing Taylor-Couette flow with suction. *Phys. Fluids* **22**(3) (2010) 034105.
[12] R. R. Kerswell, Instability driven by boundary inflow across shear: a way to circumvent Rayleighs stability criterion in accretion disks? *J. Fluid Mech.* **784** (2015) 619–663.
[13] M. Gellert, M., G. Rüdiger, Stratorotational instability in TaylorCouette flow heated from above. *J. Fluid Mech.* **12**(8), 1955-1968 (2000).
[14] G. S. Beavers, D. D. Joseph, Boundary conditions at a naturally permeable wall. *J. Fluid Mech.* **30**(1) (1967) 197–207.
[15] R. Temam, X. Wang, Remarks on the Prandtl equation for a permeable wall. *Z. Angew. Math. Mech.* **80** (2000) 835–843.
[16] K. Ilin, Viscous boundary layers in flows through a domain with permeable boundary. *Eur. J. Mech. B/Fluids* **27** (2008) 514538.
[17] V. I. Yudovich, Rotationally symmetric flows of incompressible fluid through an annulus. Parts 1 and 2. Preprints VINITI no. 1862-B01 and 1843-B01, 2001 (in Russian).
[18] M. V. Korobkov, K. Pileckas, V. V. Pukhnachov, R. Russo, The flux problem for the Navier-Stokes equations. *Russian Mathematical Surveys* **69**(6) (2014) 1065–1122 (translated from *Uspekhi Mat. Nauk* **69**(6) (2014) 115–176).

[19] S. N. Antontsev, A. V. Kazhikhov, V. N. Monakhov, *Boundary value problems in mechanics of nonhomogeneous fluids* [translated from the Russian]. Studies in Mathematics and its Applications, **22**, North-Holland Publishing Co., Amsterdam (1990) 309 pp.

[20] A. B. Morgulis, V. I. Yudovich, Arnold's method for asymptotic stability of steady inviscid incompressible flow through a fixed domain with permeable boundary. *Chaos* **12** (2002) 356–371.

[21] P. Billant, F. Gallaire, Generalized Rayleigh criterion for non-axisymmetric centrifugal instabilities. *J. Fluid Mech.* **542** (2005) 365–379.

[22] N. S. Barlow, B. T. Helenbrook, S. P. Lin, Transience to instability in a liquid sheet. *J. Fluid Mech.* **666** (2011) 358–390.

[23] M. Abramowitz, I. A. Stegun, (Eds.) *Handbook of Mathematical Functions: With Formulars, Graphs, and Mathematical Tables*. Dover, New York (1964) 1046 pp.

[24] K. Ilin, A. Morgulis, On spectra of open flows of an ideal fluid in annular domains. In *Studies in mathematical analysis, differential equations, mathematical modelling and their applications*. Vladikavkaz: South Mathematical Institute of RAS (2014) pp. 408–419 (in Russian).

[25] G. Pólya, G. Szegö, *Problems and Theorems in Analysis II: Theory of Functions. Zeros. Polynomials. Determinants. Number Theory. Geometry* (Vol. 2). Springer (1976).

[26] G. Pólya, Über die Nullstellen gewisser ganzer Funktionen. *Mathematische Zeitschrift* **2**(3) (1918) 352–383.

[27] A. Meseguer, L.N. Trefethen, Linearized pipe flow to Reynolds number 10^7. *Journal of Computational Physics* **186**(1), 178-197 (2003).

[28] T. H. Hughes, W. H. Reid, On the stability of the asymptotic suction boundary-layer profile. *J. Fluid Mech.* **23**(4) (1965) 715–735.

[29] L. M. Hocking, Non-linear instability of the asymptotic suction velocity profile. *Quarterly Journal of Mechanics and Applied Mathematics* **28**(3) (1975) 341–353.

[30] C. R. Doering, E. A. Spiegel, R. A. Worthing, Energy dissipation in a shear layer with suction. *Phys. Fluids* **12**(8) (2000) 1955–1968.

[31] L. N. Howard, A. S. Gupta, On the hydrodynamic and hydromagnetic stability of swirling flows. *J. Fluid Mech.* **14** (1962) 463-476.

[32] H. P. Furth, J. Killeen, M. N. Rosenbluth, Finite resistivity instabilities of a sheet pinch. *Phys. Fluids* **6**(4) (1963) 459–484.

[33] P. Chossat, G. Iooss, *The Couette-Taylor Problem*. Springer, New York (Applied Mathematical Sciences., Vol. 102) (1994) 233 pp.

[34] V. N. Govorukhin, A. B. Morgulis, V. A. Vladimirov, Planar inviscid flows in a channel of finite length: washout, trapping and self-oscillations of vorticity. *J. Fluid Mech.* **659** (2010) 420-472.

[35] E. Kersale, D. W. Hughes, G. I. Ogilvie, S. M. Tobias, N. O. Weiss, Global magnetorotational instability with inflow. I. Linear theory and the role of boundary conditions. *Astrophys. J.* **602**(2) (2004) 892–903.

[36] V. A. Vladimirov, V. I. Yudovich, M. Y. Zhukov, P. V. Denissenko, Asymmetric flows induced by a rotating body in a thin layer. HIMSA Preprint No. 3 (2001).

[37] P. V. Denissenko, Asymmetric Flows Driven by a Rotating Solid in a Fluid Layer. PhD thesis, University of Hull (2002).